SCIENTIFIC CULTURE
www.sci-cult.com

SCIENTIFIC CULTURE, Vol. 10, No. 3, (2024), pp. 101-134
Open Access. Online & Print

DOI: 10.5281/zenodo.14274519

A FIRST USE OF THE POWER LAW AND GROWTH RATE OF EXPERIMENTALLY AGED OBSIDIAN HYDRATION FOR DATING PURPOSES: Part I

Liritzis Ioannis[1,2] and Andronache Ion[1]

[1]Alma Mater Europaea University (AMEU) Slovenska Ulica 17, 2000, Maribor, Slovenia
[2]European Academy of Sciences & Arts, St. Peter-Bezirk 10, A-5020 Salzburg, Austria

Received: 20/08/2024
Accepted: 30/09/2024

Corresponding author: I. Liritzis
(ioannis.liritzis@almamater.si; ioannis.liritzis@euro-acad.eu)

ABSTRACT

The mechanism of diffused water through the surface of archaeological Obsidian blades, in the course of time, a mainly temperature-dependent and concentration-driven phenomenon, related to the obsidian hydration dating (OHD), is a subject of ongoing development. Fourteen obsidian specimens from California, Easter Islands, and Africa of laboratory ageing and known age spanning from some hundreds to some thousands of years have been investigated. The microscope images of micro-scale thin hydration rims of naturally hydrated artifacts and experimentally hydrated ones have been processed. It has been shown that the high-temperature aged experiments data of an obsidian source (as image area in pixels and hydration depth) can be properly processed to calculate the age of an obsidian artifact derived from the same source, although it may be applied to different and distant obsidian sources.

The first novel power law approach is presented exploring various facets of the thin-sectioned images of absorbed water from obsidian surfaces.

Hydration growth rates calculated from areal pixels, a power law functional behavior of temperatures of experimentally hydrated layers with growth per year, as well as, their hydration thickness, is discussed. The obtained ages from the tentative power law equation are estimated for anticipated environmentally effective temperatures. Compatibility and differences with conventional OHD ages, reporting problematic reported data and image scaling issues, are critically discussed, maintaining the logic that the present and future application should be made on a similar or closely related source of both the sample to be dated and the experimental simulation samples at high temperatures.

KEYWORDS: obsidian hydration dating, power law, temperature, microscopic, growth rate, temperature, OHD, Arrhenius

1. INTRODUCTION

Diffusion is an essential transport mechanism in many rock and biological systems and is known to be susceptible to environmental and intrinsic structure and inhomogeneity. The most basic definition of diffusion is that it presumes a homogeneous environment with a continuously increasing mean squared displacement and a Gaussian distribution of particle displacements. When inhomogeneities exist in the environment, the connections between diffusing particulate and the mineral or cellular structure result in challenging displacement distributions, which are most widely classed as non-Gaussian (Hall and Ingo 2021).

The value of power law exponents has been proposed to construct universality classes that capture the dimensionality and type of disorder inherent in the diffusion environment (Novikov et al., 2014).

Friedman and Smith (1960) approached the dating of obsidian stone tools from the last time they were used by prehistoric people, observing that a newly exposed surface of obsidian takes on water from the environment at a known rate that can be used to calculate the time elapsed since exposure and, thus, the date of an obsidian artifact's production. Following that, the hydration technique was further investigated, and several variations of the so-called obsidian hydration dating (OHD) method were created, proposing both empirical and intrinsic rate methods. Secondary ion mass spectroscopy (SIMS) has been used over the last 20 years to properly quantify the hydration profile (water content vs depth) in a phenomenology manner. Models explaining the diffusion process are used to determine the age by modeling the hydration profile (Liritzis & Laskaris, 2021)

Even today, sixty-three years after the launch of the obsidian hydration dating approach, the precise mechanism by which water diffusion takes place in amorphous rhyolitic glass such as obsidian is still under investigation (Doremus 1969, 2000, 2002; Crank 1975, Zhang et al. 1991; Nowak and Behrens 1995; Zhang and Behrens 2000; Anovitz et al. 2006). Doremus (2000) proposed a hypothesis for water diffusion, a theoretical model known as the "diffusion-reaction model." According to the suggested model, the water in the burial environment interacts with the Si-O-Si clusters to generate silanol groups (eq. 1).

$$H_2O + \text{Si-O-Si} \leftrightharpoons 2\text{SiOH} \quad (1)$$

Additional research (Stevenson et al., 2000, 2021) revealed that the water molecules on the obsidian surfaces are the primary molecules that disperse in the obsidian interface and that the newly generated silanol groups (Si-O-H) stay stable throughout diffusion in the bulk matrix.

Water diffusion is a complicated and dynamic process at the start of the diffusion process, as evidenced by accelerating hydration tests (Anovitz et al., 2004; Stevenson and Novak, 2011; Stevenson et al., 2019). As a result of diffusion, hydration has a high surface concentration while the diffusion coefficient decreases (Liritzis 2014). Following up on Liritzis' technique, it has been proposed that this change may be due to glass surface relaxation when tension in the near-surface region is released (Liritzis 2006, 2014; Liritzis and Laskaris, 2012).

The water from the burial site is absorbed by the obsidian's surface, resulting in the production of a hydration rim at its interface layer (a few microns under the surface). The hydration of obsidians is a complex, diffusion-based phenomenon that is greatly influenced by temperature, the intrinsic (structural) water of the artifact, water concentration on the glass surface and the glass matrix and micro-crystallization but also relative humidity (RH) (Mazer et al., 1991; Liritzis et al., 2004, 2007, 2008).

The variable temperature of the burial environment and various factors participating in the diffusion process during the tool's lifetime contribute to the final shape of the diffusion profile (concentration vs depth), the SIMS sigmoid curve (Liritzis t al., 2008; Liritzis and Laskaris 2012).

For dating purposes, Friedman & Smith (1960) suggested the empirical power law equation (eq. 2):

$$x^2 = k*t \quad (2)$$

Where x is the thickness of the hydration rim in microns (μm), t is the age in years, k is the hydration rate at a particular temperature/relative humidity (Friedman & Long 1976; Liritzis 2014; Liritzis and Laskaris, 2021).

For water to penetrate obsidian, a water molecule must have enough energy to stretch the glass matrix and enter one of the spaces in between. This energy is directly related to the temperature in Kelvins, which means that the rate of hydration is dependent on temperature. The specific relationship is described by the Arrhenius equation:

$$k = A*\exp(-Q/T) \quad (3)$$

Here, A is a constant that determines the rate of hydration, Q is the energy needed to activate the process, and T is the temperature in Kelvins. The pre-exponential constant A is measured in square micrometers per unit of time, while Q and T are measured in Kelvins (which can be calculated by adding 273.15 to the temperature in Celsius). This information is based

on research by Doremus (2002) and Friedman and Long (1976).

Eq.3 is essentially the hydration rate k (μm^2/day) of Arrhenius as in eq. 4:

$$k=A*e^{-E/RT} \quad (4)$$

T is the absolute temperature (Kelvin, K) which represents the effective hydration temperature (EHT), k is the diffusion coefficient (μm^2/day), A pre-exponential replacement, as a source-specific constant, E the activation energy (joules per mole) again as a source or burial environment's constant and R the gas constant (8.314 J / mol·K joules per degree per mole). The energy has not been satisfactorily addressed as dependent on environmental context factors affecting chemical reaction, which must be considered (See **APPENDIX**, **Activation Energy**).

The primary issue in all techniques is determining the "effective temperature" T, which determines the diffusion rate. (for more on thermal history and effective temperature, see Smith et al., 2003). This is the temperature required to produce equivalent hydration rim as the fluctuating temperature over the identical archaeological duration. EHT can never be lower than the mean temperature, as per the Arrhenius equation's mathematical structure. The average temperature experienced by the artifact during its interment period is known as the burial period's mean temperature.

Using MatLab runs for typical archaeological conditions the best fit for EHT calculation was derived simplified from the equivalent equation in Rogers (2007).

$$EHT = T_a + 0.0062*(V^2_a + V^2_d) \quad (5)$$

where Ta is the average annual temperature, V_a is the annual variation (hottest-month mean minus coldest-month mean) and V_d is mean diurnal temperature (all in °C).

Three dating approaches were proposed to solve this issue, both of which sought to quantify the rate at which water diffuses through glass:

Though initially the relationship between hydration depth (as determined by microscopy, SIMS, or other means) and the ^{14}C dates were examined with which the measured obsidian samples are strictly stratigraphically associated context-wise, no any calibration was possible. Taking up this relationship Rogers and Stevenson (2023) determined Hydration rates by obsidian-radiocarbon association and the science-based model have an accuracy between 5% and 13%, based on obsidian source. Although it is possible to create an ad hoc best-fit equation from archaeological data for a specific analysis, the authors conclude there is no assurance that it will be valid beyond the data set on which it is based, and the procedure was not recommended.

So far, the main methodological dating approaches used are:

i. Following the conventional age eq (2) and calculating a hydration rate (k) of eq. 3, based on the activation E, temperature T and the Arrhenius equation for reaction kinetics (eq.4). This k value is either estimated from nearby sites of supposedly similar climatic history (Pearson 1995, Stevenson et al. 1998, 2001; Rogers 2008) or, in another approach (intrinsic rate), the k of eq. 4 is experimentally determined and coupled with accurate measurements of the site's temperature to derive an age (Anovitz et al., 1999). Aged hydration at high T for same or different obsidian sources helped calculating the rate, k. Although other equations than eq.2 have been proposed for Bodie Hills (e.g., Basgall and Giambastiani 1995; Pearson 1995), the depth is proportional to time power law t^n where t is time and n = 0.5 within limits of experimental error, i.e. the equation (2) is the only form with both theoretical (Ebert et al. 1991; Doremus 2002) and laboratory (Doremus 1994; Stevenson et al. 1998, 2000, 2021; Anovitz et al., 2004) support. Age analysis by obsidian hydration requires knowledge of the hydration rate of the obsidian, so seven methods for 26 obsidian sources for computing hydration rates were described, with mathematical details (Rogers and Stevenson 2022a). Hence, results have demonstrated that a simple square-root-of-time model of the evolution of the diffusion profile is not adequate to describe the diffusion process, as measured diffusion profiles exhibit the effects of concentration- and time-dependent, non-Fickian diffusion. This research is still going on yet the square-root-of-time model prevails.

ii. Rogers and Stevenson (2022a, 2024) tried to produce a calibration equation relating to Water content (W), EHT and K. The hydration rates computed are based on eq.3 of high T aged obsidians with various water content. The normalized activation energy, E, from equation (2), was related to W (weight percent H2Ot). Measuring water content of a specimen, either by IR spectroscopy or by the Structural Water determination method described (Rogers and Stevenson 2022b, 2023; Franchetti et al., 2024), the authors maintain that this is a simple step any archaeologist can make to improve OHD accuracy and precision following the eq. 2 again for the age estimation. When the obsidian parameters A and E/R are known, from the Arrhenius plot LnK versus 1/T, the hydration rate can be computed for any desired temperature and the dates are calculated from eq 2 and for different T.

iii. By using the idea of a surface saturation (SS) layer, and applying ion bombardment using SIMS on the surface, the obtained H^+ depth profile was fitted by polynomial functions and following the diffusion

law an age equation is produced (Liritzis and Diakostamatiou 2002; Liritzis et al., 2004; Liritzis 2014, 2006; Liritzis & Laskaris 2009; 2021). In the Liritzis' method the flux F (mass per unit area per unit time) of a substance diffusing into another substance is based on Crank's diffusion equation between concentration C, time t and diffusion coefficient D (Liritzis et al., 2004; Liritzis 2006, 2014). In the case of a semi-infinite medium with steady boundary conditions, assuming the process is pure diffusion, and no chemical reaction is taking place and the assumption that the diffusion coefficient is constant, the solution to the 2nd order partial derivative operator equation can be shown to be:

$$C = C_0 \, \mathrm{erfc}(z) \quad (6)$$

where C is the water concentration at depth x and time t, C_0 is the concentration at the surface, and erfc is the complementary error function (Crank 1975). Following Crank (1975), the argument z in eq. (6) is

$$z = x/(Dt)^{1/2} \quad (7)$$

where x is depth into the obsidian, t is time, and D is the diffusion coefficient.

Equation (7) describes the variation of concentration both in space and time. The hydration front is usually defined as the point where C/C_0 reaches some set value, or in other words the point where z equals a constant. This is the surface saturation (SS) point close to surface (SIMS-SS method, Liritzis 2006, 2014; Liritzis and Laskaris 2012).

Equation (7) can then be rearranged as in eq.2 the form familiar from hydration studies since Friedman and Smith (1960).

The SIMS-SS method and criteria of suitability has had several World applications (Liritzis and Laskaris 2009; Liritzis et al., 2008).

Regarding the burial temperature and hydration rate Rogers (2007) computed an effective hydration temperature from a numerical integration of the hydration rate over the temperature model determining an EHT for each artifact, based on site elevation and burial depth, and applied a rim correction factor (RCF) to correct the rim value to a consistent reference temperature. For the hydration rate for Bodie Hills (BH) obsidian at 20°C a value of 14.31 μ^2/1000 yrs was reported. The computed ages of the specimens from this region are compared with the calibrated radiocarbon ages so this is a per case issue. The standard deviation of the percentage error was relatively large, 23%. In fact, approximately half of this deviation is attributable to EHT errors, with the remaining most likely reflecting the poorly known chemistry and variability of Bodie Hills obsidian (Rogers 2008b). Given the current level of knowledge of Bodie Hills obsidian, it would be imprudent to assume an accuracy greater than roughly 20% in doing chronometric studies, according to Rogers (2008b).

At any rate, the effect of temperature on hydration rate is significant and the result of the hydration layer expressed in terms of pixels and fractals is still an ongoing development.

An earlier investigation on the variations of water and structural entities within the obsidian in the micron and nanoscale of divided hydration and pure obsidian using fractals (Liritzis et al., 2024) indicated interesting aspects of hydration medium and waterfront tail. A fractal variation along the hydration layer which mirrors somehow the S-like H^+ concentration changes at depth.

The present work focuses on the growth rate and its power law dependence of water in obsidians in various controlled temperatures extrapolated to environmental temperatures, as well as on archaeological hydrated blades. Making use of the obtained rates tentative dates for five known age obsidian artifacts are made.

The goal here is to investigate a) the functional dependence of obsidian hydration growth as a function of temperature, b) the comparison between different laboratory-aged obsidians at 140-180°C and 160°C /30 days and 180°C/60 days, the respective hydration layer pixels of which are standardized in growth rates per day, and c) the extrapolation from high T °C to ambient temperatures (10-30 °C) and use of these temperature values to recalculate the known ages based on normalized areal pixels, but also on the growth rate of hydration thickness per year.

The approach also points the way to an interesting new research direction in obsidian hydration dating studies. We understand the limited number of cases in the use of data and therefore we consider the effort a first step towards further deepening.

MATERIALS AND HYDRATED IMAGES

Fourteen obsidian samples were processed. For abbreviations of their initials are used throughout the text. of Five (5) images of an obsidian source from Bodie Hills (BH1), California that have been experimentally hydrated from 140, 150, 160, 170, 180°C for 59.22 days (Fig.1) (Stevenson, CM pers. communication; Hughes 1984).

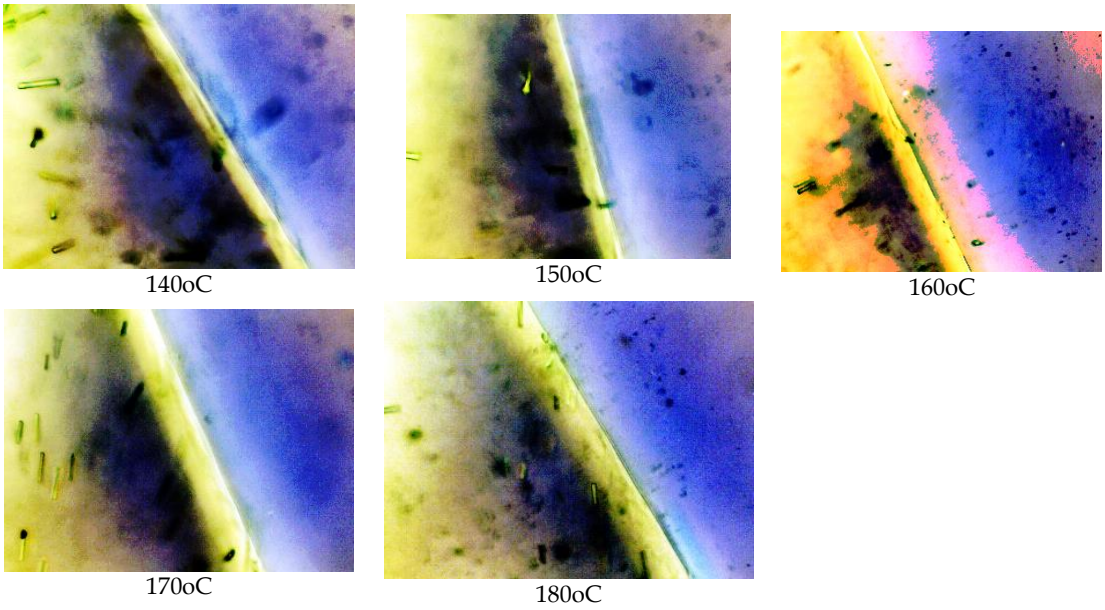

Figure 1. Bodie Hills data (BH1). The five hydrated zones per laboratory experimental temperature for 59.22 days. The narrow yellowish zone is the hydration layer and on the right is the surface and the glass support (bluish), and on the left (darker) the inner obsidian. The thickness (μm) per temperature: 140°C (5.91um); 150°C (7.75um); 160°C (9.96um); 170°C (13.29um); 180°C (18.09um).

The BH source has proved most troublesome with traits consisting of two distinct forms. One gray-green bands intersected with much smaller quantities of clear bands containing black and white phenocrysts, and the other very dense black, red brown dendritic masses (see Bettinger et al., 1984).

Two (2) African blades PE-21 and PE-23 (Fig.2) are coming from a cave in Africa of the Middle Stone Age Ethiopian rock shelter of Porc Epic which is supposed to date to approximately 60-70kya (Clark et al., 1984).

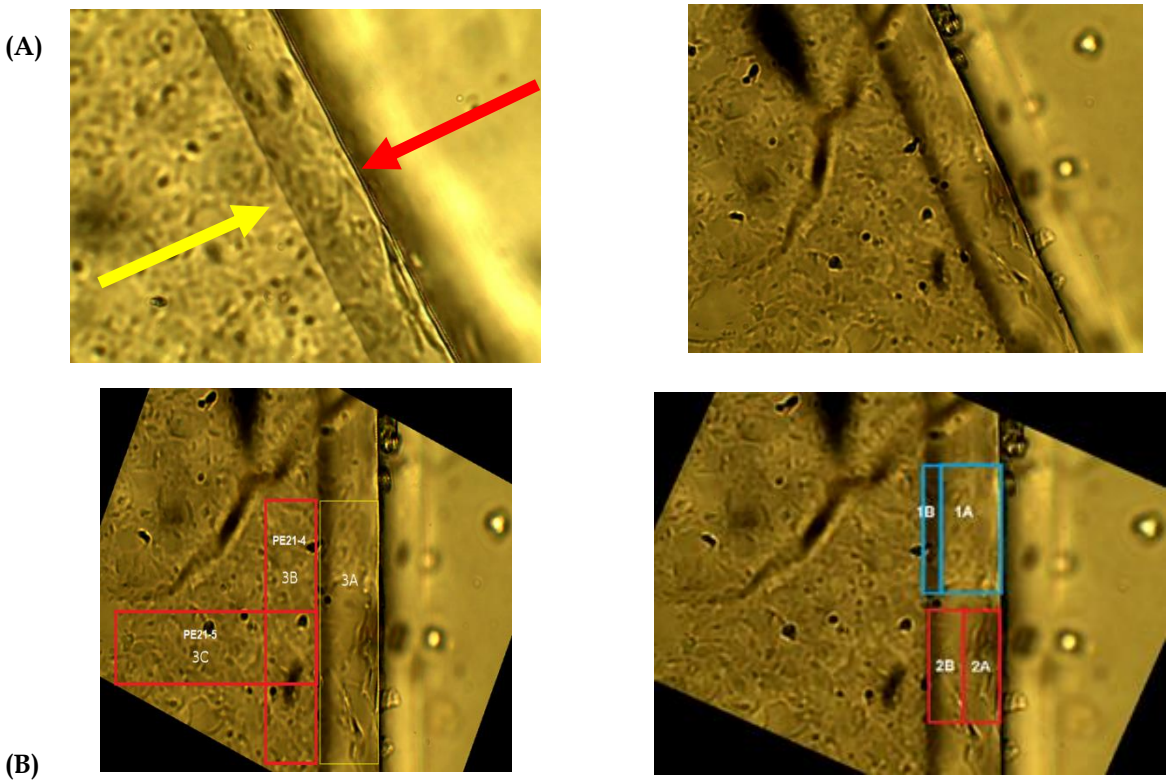

Figure 2. Porc Epic obsidian hydration layers of a) PE 23, and, b PE-21 and areas measured by fractals and pixels.

The dark line on the surface of the layer has an optical effect. Optical thin sections were prepared, and the hydration rims were photographed with a Motic 2MB digital camera mounted on a Motic polarizing microscope at a magnification of 600x. The darker part near the diffusion front may be a difference in the refractive index of the glass but also lighting intensity. The refractive index of the layer is much higher than the bulk glass (~1.56 vs ~1.49). In fact, when a hydration layer is viewed with polarized light under crossed-Nicols a gradient can be seen in this region, but the birefringence intensity cannot be reliably tracked with distance.

Two (2) Orito Obsidians, Easter Island (Orito) source, heated at 160°C/ 30 days and 160oC / 50 days Fig.3) (Tom Origer, pers. data).

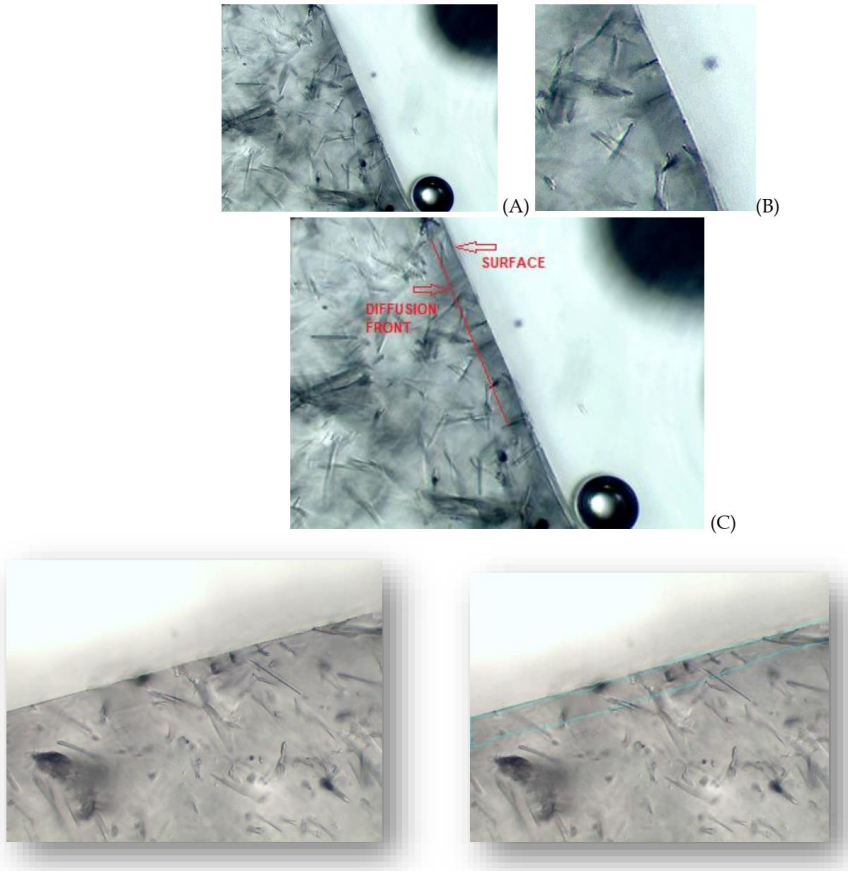

Figure 3. Orito Easter Island blades. RBC-600, hydrated layers for a)160 °C / 30 days enhanced, b) cropped, c) surface and diffusion front, and d) RBC-601, for 160 °C / 50 days; blue lines indicate the layer. (not in scale, pixels normalized to NV or BH of same area)

Five (5) Napa obsidians from Napa Valley (NV) in northern California: NV-1.9, NV-2.8, NV-4.5, NV-5.9, and NV-7.7 (NV stands for Napa Valley and the number of hydration layers in microns). Three have been dated to: NV-1.9 472, 2650, and 7750 years old, found at different depths below surface ground. O-1346#27, 0-10 cm(17.15 °C estimated by Rogers, pers. Comm.[1]) O-1346#37 at 20-30cm, (16.23 °C estimated by Rogers); and O-1346#56 at 90-100cm (15.76 °C estimated by Rogers) (Tom Origer pers. Communication).

The two NV-2.8 and NV-5.9 are experimentally hydrated at 150°C / 10 days and 140°C / 60 days respectively. (Fig.4) (Hughes 1984)

The NV-5.9-micron specimen is from the same Napa Valley obsidian rock as the specimens with 1.9, 4.5, and 7.7 micron measurements.

[1] The EHT has been calculated by Rogers from WRCC temperature data for St Helena and Calistoga and computed temperature model parameters. The parameters for the 2 sites were close but not identical, so he used the average. Then he made the adjustment for burial depth and computed EHT.

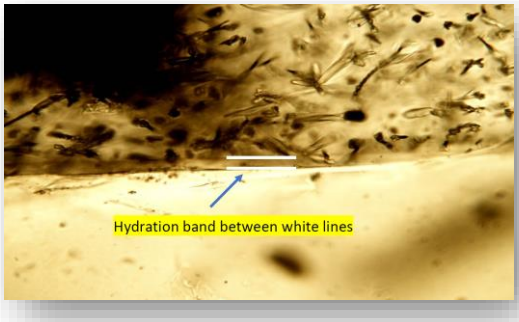

(A) NV-4.5

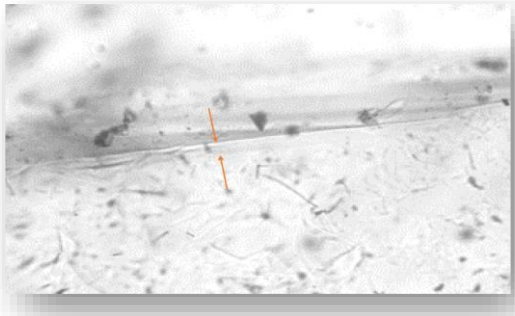

(B) NV-5.9

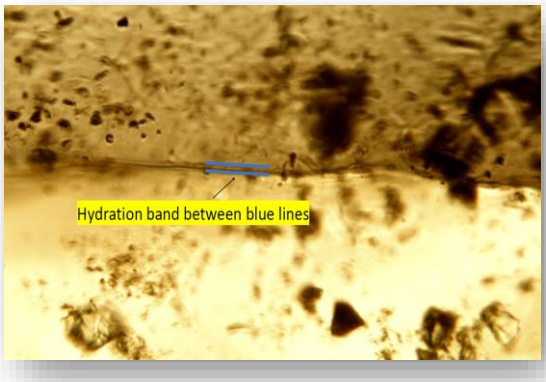

(C) NV-1.9

(D) NV-2.8

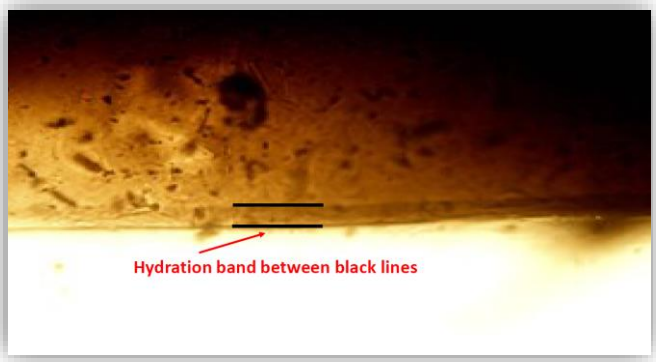

(E) NV-7.7

Figure 4. Napa Valley hydration layers A) Slide O-1346 #27, 4.5 microns hydration rim Napa Valley of 2,646 years, B) NV-5.9. Here is an image of a hydration band (between the orange arrows) that measures 5.9 microns. It was created at a temperature of 140 degrees Celsius for a period of 60 days, c) NV-1.9, Slide O-1346 #37, 472 years, D) NV-2.8, 2.8 micron hydration on obsidian in our lab for periods of 10 days at 150°C, (E) NV-7.7, Slide O-1346 #53 7.7 micron 7,747 years (scale replaced by rim reading).

2. METHODS

All the analyzed images were manually segmented, extracting only the hydration belts. The resulting images were then binarized: hydration belts were represented in white pixels, while the glass and body of obsidian were represented in black pixels (Schindelin et al., 2015; Schneider et al., 2012) (see, Fig.5). The detailed protocol of these processes is given in **Segmentation and binarization protocol using ImageJ 1.54 open source based on java software**, **APPENDIX.** The images provided were not all scaled and rescaling was applied based upon a reference image. This induces some uncertainties which are taken into account in the final drawn conclusions in the estimation of the dates. In future calibrated images are most needful.

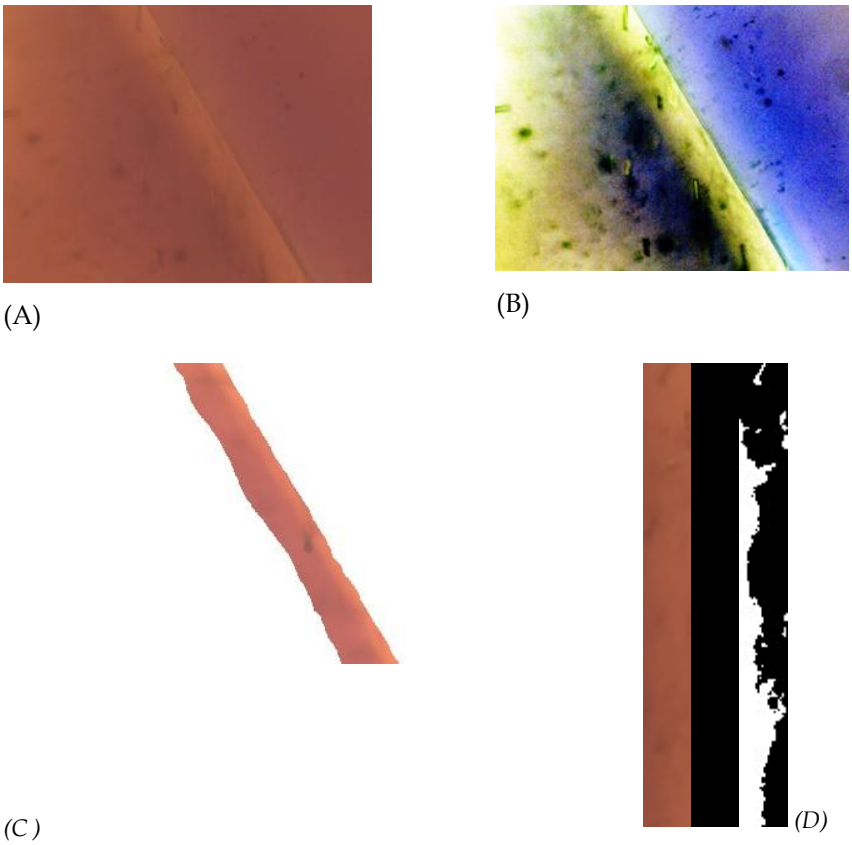

Figure 5. A) the original image from the microscope for the 180°C sample, BH B) Lookup Table (LUT) for original image, A, to identify better the hydration belt for segmentation, C) the segmented image, of (A) using (B), and D) rotated hydration belt (left brown), binarized (center black) and potential water (right), depicted by black pixels.

The number of pixels for each hydration belt was extracted. Subsequently, the total number of white pixels (representing hydration belts) in the images was quantified.

All images were normalized to Napa Valley because the size of images was of different size. Napa Valley 1429*1072 pixels were preserved (because were the biggest images as size). The African 800*600 were rescaled to 1429*1072, the Orito 800*600 were rescaled to 1429*1072 and the Bodie Hills 320*240 were rescaled to 1429*1072 pixels. All these operations were performed using the open-source software ImageJ 1.54f (Pearson, 1995; Stevenson et al., 1998; Rogers, 2008a). (see: APPENDIX Fig.A1, Fig.A2. Table A1 gives a summary of all obsidians studied hydration belts and the hydration layers and percentage of full images for the 14 samples. All images were rescaled to 1429*1072 according to Napa images).

In parallel to image pixels, depth data regarding the thickness in microns of the hydration belts were used.

The dating of the age of the obsidian samples was done based on two alternative approaches. A) power law equations, and B) growth rate calculations.

Power law: Power law indeed represents a mathematical relationship where a change in one quantity is proportional to a power of the change in another quantity, regardless of their initial values. This means that one quantity varies as a power of the other, and the exponent in the power law equation determines the nature of this relationship. We used power trendline from Microsoft Excel. A power trendline is a curved line that is particularly suitable for data sets where measurements increase at a consistent rate.

The formula of power law is:

$y = ax^b$ (8)

"y" represents the dependent variable, (pixels/yr or microns /yr (vertical axis).

"x" represents the independent variable, Temperature (horizontal axis).

"a" is the coefficient.

"b" is the exponent or power.

The values of "a" and "b" are determined by Excel based on the data points to provide the best fit for the power trendline. One can use this formula to make predictions or analyze the relationship between our variables.

Growth rate: The growth rate, denoted as "Gr" is a measure used to quantify the rate at which a specific quantity, such as in our present case the hydration layer in pixels, increases or decreases over a particular period. It is typically expressed as a percentage or a decimal and indicates the relative change in the quantity's value over time. The growth rate can be calculated using the following formula:

$$G_r = \frac{Increase\ of\ hydration\ quantity\ for\ T2}{original\ hydration\ quantity\ for\ T1} \quad (9)$$

Hence, for the following developments the respective Gr should be Tn/Tn-1, where T is the time or temperature quantity. This formula gives the rate of change as a proportion of the initial quantity. If expressed as a percentage, one can multiply the result by 100 to obtain the percentage growth rate. The growth rate is defined as the ratio of pixels for successive agents of temperature or dates over the pixels of immediately earlier agent. A relevant term is the hydration rate which for its computing in earlier times scholars were based on the classic method by obsidian-radiocarbon association (Basgall 1990).

The power law of eq.8 was applied on the Bodie Hills five experimentally aged data and on the three Napa Valey archaeological samples. Here two approaches were made for both case studies: the experimentally aged temperature data (at high temperature) were plotted versus pixels per year (the time parameter comes in from the growth of the hydration layer for a specific duration in days). The power law derived from the 3 and 5 data points respectively was extrapolated back to environmental ambient temperatures, which are met usually in buried archaeological blades (10-20 ^{o}C), assigning to these temperatures certain values for pixels/yr and microns/yr.

The Gr was applied to the two Orito, two NV experimentaly aged and three NV archaeological samples, and the five BH aged samples.

3. RESULTS

3.1 Hydration layer dependence on Temperature of Bodie Hills (BH)

The hydration belts experimentally hydrated in five temperatures (T) for a time of ~2 months from BH have been analyzed in total pixels for the whole hydration belts, 3A of Fig.2. The results are shown below (Fig. 6) indicating higher water per increased T. (See **APPENDIX on Growth rates of BH data, Table A3**). The cumulative growth rate of water due to higher temperature is ranging between 1.1 to 2.1 pixels / ^{o}C and average ~1.6 pixels/ ^{o}C (Fig.6).

In the single growth rate per temperature, it is interesting to note the 170 ^{o}C turn over point with a lower rate at next 180^{o}C hydration. The inconsistency might be due to some degree of inhomogeneity of BH source (Bettinger et al., 1984).

The pixels at 60days were converted to pixels per day eventually per year. The functional behavior of the five temperatures versus hydrated layer pixels /year was made applying four fitting functions (polynomial, exponential, linear, power law). We adopt the power law as the most appropriate complying with the empirical age equation (Fig.7) (see above Introduction and **APPENDIX** for the respective functions **Fig.A1** and **Table A1**).

The power law of equation (10) for BH experimental data is used to estimate hydration ages of known age archaeological obsidians (below).

$$A=0.0006*T^{3.2},\ R^2=0.92 \quad (10)$$

where A the area in pixels/yr and T the temperature.

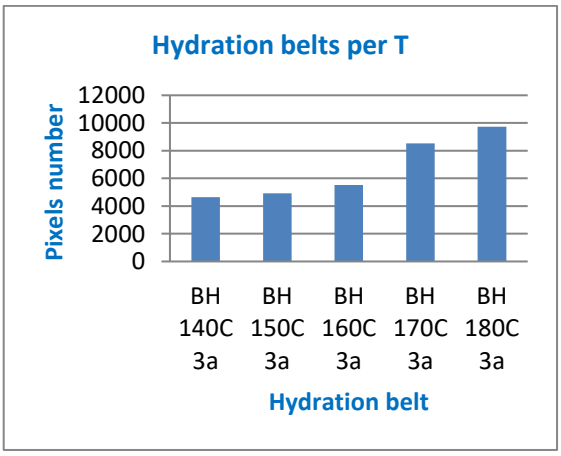

(A)

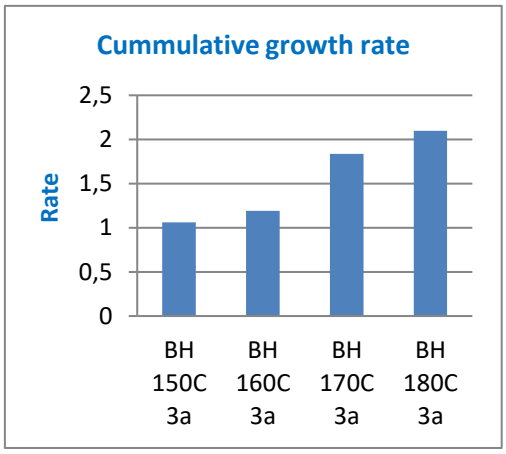

(B)

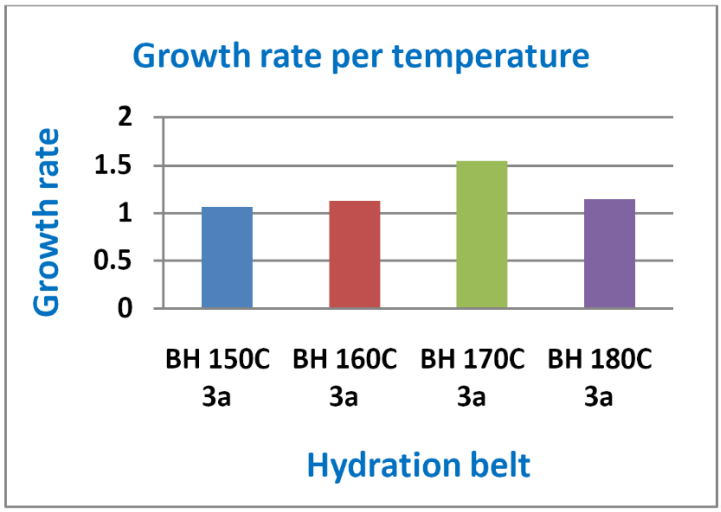

(C)

*Figure 6. A) The five hydration belts (3a only hydration rim as in Fig.2) per temperature, versus total pixels, B) Cumulative Growth rates for t=~60 days hydration, as BH150/BH140; BH160/BH140, BH170/BH140 and BH180/BH140. C) Growth rate per temperature for t=~60 days hydration as BH150/BH140; BH160/BH150, BH170/BH160 and BH180/BH170. The hydration belts 3a and growth rates were normalized. The original size of BH images 320*240 (76800 pixels) were rescaled to the size of 1429*1072 Napa Valley (NV).*

It is of interest the temperature T quadratic dependence (and significance) from hydration rim parameter of pixels / year. Physics and chemistry of the diffusion process suggests that the relationship between age (t) and rim thickness is also expected to be approximately quadratic, i.e., of the form of eq. (2). In eq.10 the quadratic relationship has an exponent 3.2. (see, Rogers 2006; Liritzis et al., 2004).

Different approaches lead to similar forms have suggested that power laws, and particularly the values of power law exponents, capture a fundamental property of the observed dynamics. It has been proposed that the value of power law exponents defines universality classes capturing the dimensionality and type of disorder present in the diffusion environment (Lee et al., 2020). In rheological properties of minerals and rocks power law of exponent 3-5 has been reported (Karato 2013), and in biological systems (Novikov et al., 2014).

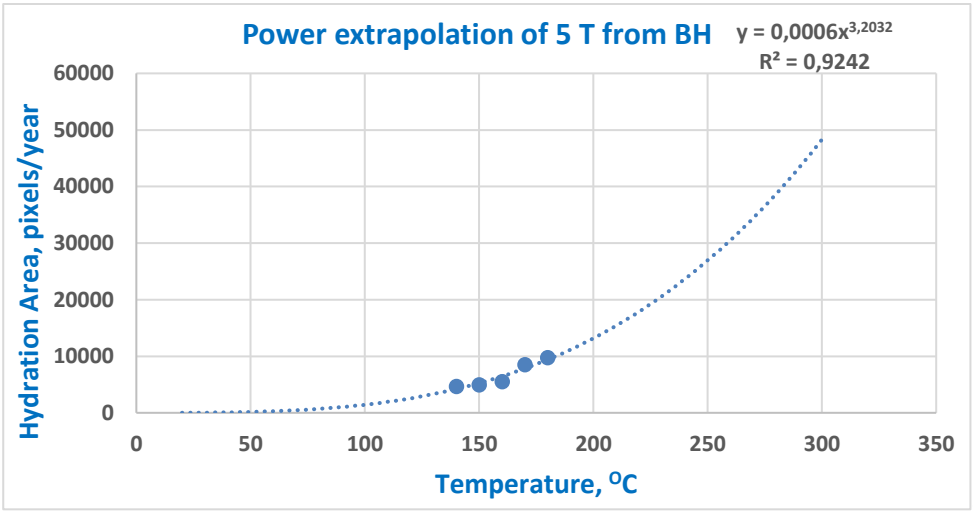

(A)

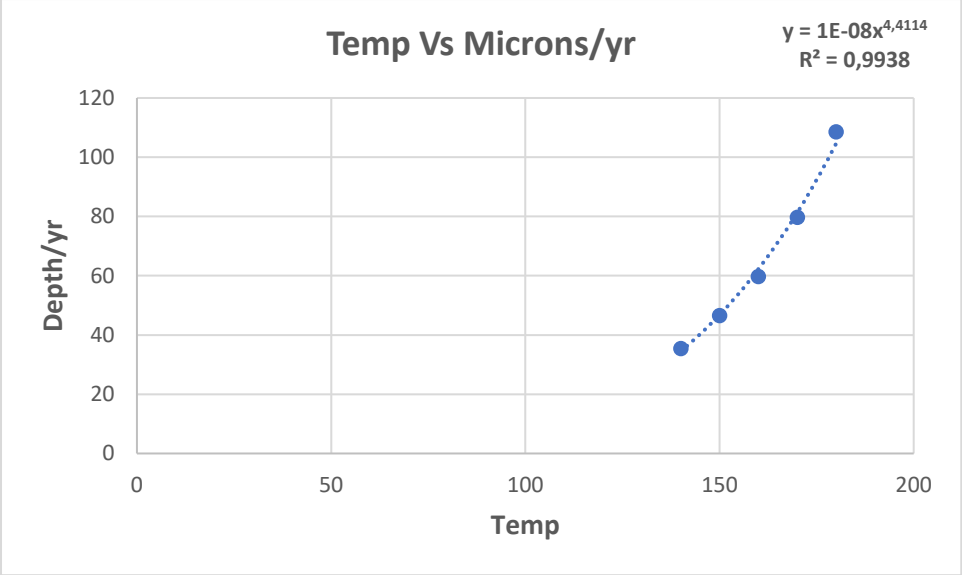

(B)

Figure 7. A) Power law for the five BH blades aged at five aged temperatures versus hydration layer in pixels, the dashed line represents mathematical reconstruction of power law behavior and on top are placed the five experimental points, B) microns/yr versus Temp of power law from the 5 temperatures of BH.

Indeed, from Fick's law of diffusion, the water diffusion is concentration driven process and depends on environmental temperature (higher temperature longer hydration rims). That is the diffusion front advances inside the obsidian carrying the water content deeper distances from surface. What the simulated high temperature (than environmental ones) does in short laboratory time, does the much lower natural environmental temperatures in time.

In accord with Rogers & Yohe (2011) the determination of a hydration rate is not a *regression* problem, but a problem of *parameter optimization*. Regression is a technique to estimate to what extent one variable depends on another. In the obsidian hydration the degree of dependence is fully known as a priori from physics, so the problem is of *optimizing a parameter* (the rate) which defines the fit between data and the physical model. This concept of this has been explained in Liritzis (2006) attributing optimization of diffusion process throughout the time (the obsidian blade was buried) to the S-like curve of H+ profile as recorded by SIMS. There the surface saturation layer was introduced. In the present work the optimization parameter is taken the *hydration rim/belt area* measured in pixels. The obtained power law is corroborated below with Orito (Easter islands) and Napa Valley (California) experimentally aged samples.

In addition, the correlation of pixels versus hydration thickness for BH contributes to understanding the growth rate per temperature and hydration layer (Table 1).

We have rescaled to squares of (thickness)^2 instead of rectangular areas.

Table 1. BH1 data hydration layers and percentage of full images and respective hydration depths in microns. All images were rescaled to 1429*1072 according to Napa Valley images using Scale algorithm from ImageJ.

Samples	width	height	Total	Hydratic belt	% hydration belt from full images	Thickness, μm/60 d
SBH 140C SA 13J	1429	1072	1531888	92518	6,030	5.91
SBH 150C SA 13J	1429	1072	1531888	98330	6,42	7.75
SBH 160C SA 13J	1429	1072	1531888	110209	7,19	9.96
SBH 170C SA 13J	1429	1072	1531888	169952	11,09	13.29
SBH 180C SA 13J	1429	1072	1531888	193866	12,65	18.09

3.2 The power law function of temperature versus hydration layer

3.2.1 Orito (Eastern Islands)

The Orito (Easter Islands) obsidians were aged at 160°C for 30 and 50 days. These Orito images were at different size compared to BH1 images and were normalized to BH values. The total hydration area of these Orito aged obsidians normalized and the growth rate per day and 60 days provides interesting results (Table 2).

TABLE 2. Orito aged obsidians with hydration layers normalized to Bodie Hills (BH) data, the total hydration layers in pixels normalized to BH of same area, the pixels of Orito hydration layers, the pixels/day, estimated pixels per 60 days per Orito sample, and respective pixels values deduced from BH data.

	Total pixels normal. to BH1 same area	Hydration layer, pixels/time	Pix/day	Est. Pix/60d	Power law from BH1 160°C & 170°C
RBC-600 Optical 160°C /30 day	76800	4185	139	8370 (lin.)	8370 (at 170°C)
RBC-601 Orito 160°C /50 day	76800	5458	109	6550 (almost non-lin.)	6893 (at 160°C)

The difference in the hydration area of 60d for the two samples RBC-600 and RBC-601 of same Orito (Easter Islands) obsidian source, rescaled to the same hydration time, is significant and around 35%. This is due to the non-linear development of diffusion advancement by temperature as is known from other studies (e.g. Ficks law) (Crank 1975). This satisfies however the result obtained with the Power law behavior of temperature against hydration growth and for two distant sources like Easter Islands and California.

In fact, the hydration layer size of RBC-600 at 60 days in 160°C, becomes larger and like the respective BH heated at 170°C. This is explained from the growth (diffusion rate) which is more accelerated, because in linear behavior it derives from the double linear result of 30x2=60 days equivalent to 4185x2=8370 pixels. It is anticipated that this linear dependance of hydration when compared with the applied power law gives the same result of 8370 but for 170oC. Also, the faster accelerated rate in the first 30 days (139pix/d for the 30d experiment) with respect to 50 days experiment reduced to 60d (109pix/d*60) confirms the similar outcome in the starting growth rate in any obsidian hydration experiment either in nature or the laboratory. Thus, in the following 30 days of the 60 days experiment, the rate is expected lower due to non-linear development, in the order of 79pix/day (thus, 79*30d + 4185=6550).

This is an excellent result which supports power law and the little significance of obsidians coming from different sources, at least, as here are the far apart Easter Islands and California.

3.3 Estimating hydration age from power law of T against hydration belts of BH

3.3.1 Napa Valley, California

The variation of the hydration belts pixels for the five obsidian blades (three archaeological of known age and two aged at 140 and 150oC) is given in Fig.8 with an expected variation between the different hydration thicknesses.

The normalized images of Napa Valley (NV) samples for width, height and total pixels are given in Table 3.

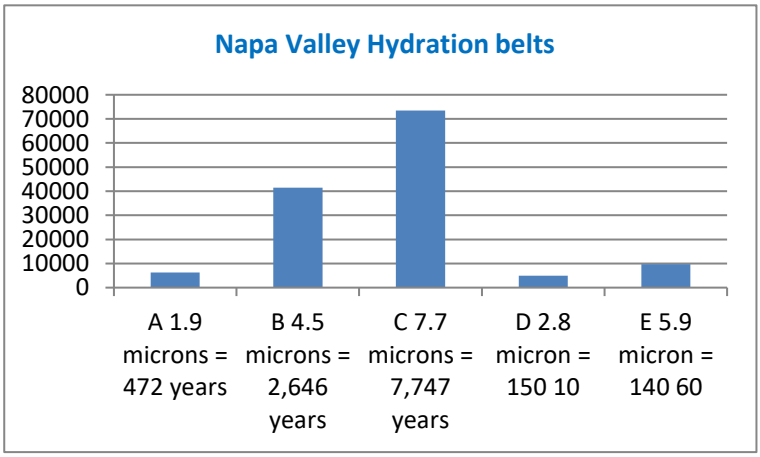

*Figure 8. Hydration belts pixels for the five obsidian blades (three archaeological of known age and hydration thickness 1.9micron, 4.5 micron and 7.7 micron, and the two aged at 140 °C and 60 days and 150°C for 10 days. (Normalized images of 1429*966 pixels for Napa Valley)*

*Table 3. Normalized images of 1429*1072 pixels for Napa Valley for the three ages and the two experimentally aged samples at 150oC/10d and 140oC/60d*

Samples	width	height	Total, pixels	Hydration belts, pixels
A 1.9 microns = 472 years	1429	1072	1531888	6243
B 4.5 microns = 2,646 years	1429	1072	1531888	44448
C 7.7 microns = 7,747 years	1429	1072	1531888	79989
D 2.8 micron = 150°C, 10d	1429	1072	1531888	3989
E 5.9 micron = 140°C, 60d	1429	1072	1531888	9409

For the three known ages samples an alternative estimation of these age was applied: **first,** following the average growth rate of experimentally aged NV samples, **second,** based on the power law of temperatures of BH data (Fig.7) and **third,** through the power law as Depth (microns)/year, without normalization, and produced ages per the T range of 10-30°C. In addition, these three NV ages were fit with four functions linear, exponential, logarithmic, and power law and used for the dating of the Ethiopean samples (Fig.9).

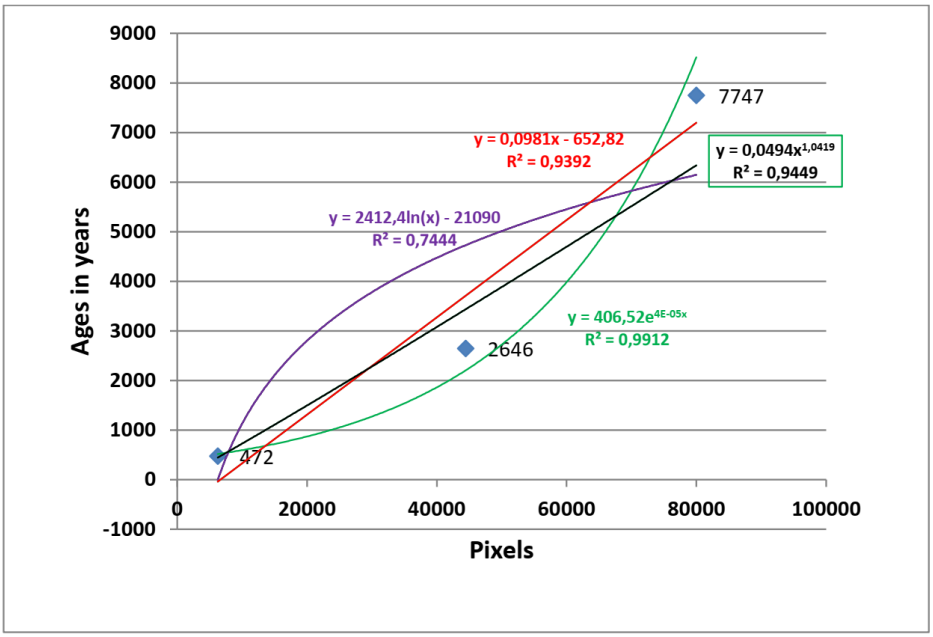

Figure 9. Napa Valley. The three ages were fit with four functions linear (red), exponential (green), logarithmic (mauve), and power law (black).

We keep the power law of the three archaeological NV samples, eq. (11):

$$A = 0.0494*x^{1.042},\ R^2 = 0.9449 \qquad (11)$$

where A is the age and x the number of normalized pixels, which is used below for calculation of the two African cases.

First, the calculated archaeological ages were based upon the **growth rate data** of the pixel/year of the 2 NV experimentally aged ones. The age difference lies between -6%, +16.4% and -26.5%, which when errors of original ages is considered this deviation becomes much lower in the order of 5-10% (Table 4).

*Table 4. A) Napa Valley three ages (left column a, b, c) and two aged data (left column d,e). Estimation of the three ages and virtual age for the aged samples. The average growth rate of pixels/year for the three archaeological artifacts and the aged ones, the average pixels/year of 2 aged ones, 3 archaeological ages and both 5 cases, their respective hydration rims and % age deviations from original OHD. B) ages computed from hydration rates and eq.2 by Rogers and Stevenson 2022a, for 16, 20°C (red) and 18°C green, being the closer ages to the reported. * Based on growth rates of the two aged values 14.05; these are hypothetical ages if these samples were hydrated in nature under certain environmental temperatures.*

Sample NV in µm	Total Norm. pixels	Gr (Norm. pixels / age), pix/year	Known ages yrs, BP	Computed ages from BH, eq.10	Computed age based on Gr of 2 aged (NV)	% Deviation between Gr and known ages
A:1.9	6243	13,2	**472**	See Table 5 below	**444**	**-6.0**
B:4.5	44448	16,8	**2646**		**3164**	**+16.4**
C:7.7	79989	10,3	**7747**		**5694**	**-26.5**
D: 2.8 µm, 150/ 10 days	3989	14,3			296*	
E: 5.9 µm, 140 /60 day	9409	13,8			699*	
		Av. of 3: 13.5				
		Av. of 5: 13.7				
		Av. of 2: 14.05				

(B)

Temperature °C	Rate (µm²/1000 years)	1.9µ, 482 yr	4.5µ,2646 yr	7.7µ, 7,747yr
20	9.889	364	2045	5990
18	7.763	468	2609	7641
16	6.073	594	3336	9764
14	4.735	768	4308	12536
12	3.679	1000	5502	16114

The Gr of the average pixels per day for D and E in Table 4 was computed using total pixels /10days or per 60 days. The results were for D = 399 pix/day = 20pix/day according to BH and for E = 157 pix / day =8pix/day according to BH. This implies that the increase of 10oC increases x2.5 the hydration rate, which in tur n is reflected in the ratio of the "virtual age" estimation for D and E (681/278=2.44).

The faster the process the greater the Gr. In fact, the growth rate slows down over time (potential oversaturation), which implies that the hydration belt does not expand as readily as it did in the early years. In actuality, the glass matrix is hydrated by water molecules permeating it, which results in expansion of the hydrated layer. The volumetric expansion of the glass during the relaxing phase that releases the internal tension makes the stress a function of the viscosity of the glass (Rogers and Stevenson 2017, 122). Since relaxation is time-dependent, the apparent hydration rate at a given temperature changes over time before reaching a constant state.

This relaxation process is linked to the surface saturation (SS) (Liritzis 2006, 2014) which keeps shifting slowly to the internal and stabilizes with entering molecules passing through to the interior and moving the diffusion front to even deeper depth.

It is observed that 7.11 and 1.8 are the Grs between B and A; and C and B respectively (it is from Table 3: B / A = 44448/6243 = 7.11 and C / B= 79989 / 44448 = 1.8).

The Gr of 7.11 applies to the interval ~500-2600yrs, which in the earlier period 2600-7700 years BP falls to 1.80 implies that in the initial time of some 100s of years the water reaches quickly the SS saturation layer (SS=surface saturation) (Liritzis 2006; Liritzis and Laskaris 2020); in later older times it becomes slower. For the 472 to 7750 years BP the 12.8 is full growth rate deriving from 7.12 x 1.80.

Second, the three Napa Valley ages are calculated from the BH rates. The ages for Napa from BH pixels /yr are given in Table 5 below for different environmental temperatures, and a satisfactory result is obtained for certain temperatures.

Table 5. NV ages from data of BH power law of T versus normalized pixels of Fig.7A. The pix/yr (fourth row) for the BH power law eq.10 is calculated per temperature and used with the normalized pixels in the three hydrated images of NV samples (fifth row). Red numbers are ages in agreement to the known calculated ones. The difference in estimated temperature between Rogers and ours is a constant deviation ca. 3.2-3.7°C.

Temp. of NV	pix/60 d, BH	pix/day, BH	pix/year, 5 points of BH (Fig.7A)	NV Pixels norm. to BH	NEW NAPA AGE, power law for the BH 5 points years BP	Known Age for NV, BP
10	0.96	0.016	5.83	6243	1071	472
				44448	7627	2646
				79989	13726	7747
11	1.30	0.022	7.91	6243	789	472
				44448	5620	2646
				79989	10115	7747
12	1.72	0.029	10.45	6243	597	472
				44448	4253	2646
90-100cm/15.76 °C by Rogers				79989	**7654**	**7747**
13, 20-30cm, 16.23 °C by Rogers	2.22	0.037	13.50	6243	**462**	**472**
				44448	3291	2646
				79989	5923	7747
14	2.81	0.047	17.12	6243	365	472
0-10, cm, 17.15 °C by Rogers				44448	**2596**	**2646**
				79989	4672	7747
15	3.51	0.059	21.36	6243	292	472
				44448	2081	2646
				79989	3745	7747
20	8.82	0.147	52.80	6243	118	472
			52.00	44448	842	2646
			52.80	79989	1515	7747

Last, the **third** alternative is the use of **power law correlation between depth in microns/year** versus Temperature for BH, to calculate the ages of Napa Valley. From Fig.7B the new power law is:

$$y = 1E\text{-}08 * x^{4.411} \quad (12)$$

where Y=depth/yr and X=Temp.

The unit of distance (micron) is the same value in thickness no matter of the size of the hydration image, while the different image resolution in pixels needs always normalization for comparative reasons.

The calculated ages (Table 6) using eq.12 correspond to 14-18°C compared to the reported ages and more calibrated than the power law of T Vs pix/yr above. The ages are closer to the reported dates and to the respective temperature by Rogers (15-16°C (earlier value Table 5 is 14°C) Vs 17.16 by Rogers, 13.7-14°C (earlier 12°C) Vs 15.6 °C by Rogers, 18-19°C (earlier 13°C) Vs 16.2°C by Rogers).

Table 6. Calculated ages of NV based on the power law of BH correlation between depth in microns/year and the temperature from the BH aged experiments (from Fig.7), without normalization, using only data in microns of the thickness. For 14-18°C shaded area the respective calculated ages in bold red are compared with the reported ones (472, 2646, 7747 years BP with an attached error ±20%).

Temp of BH experiment		**472 yr**	**2646 yr**	**7,747yr**
T	**microns/yr of Power Law of BH per Temp**	**Calc Ages, 1.9 microns/micr.yr^{-1}**	**Calc Ages 4.5 microns/micr.yr^{-1}**	**Calc Ages 7.7 microns/micr. yr^{-1}**
10	0,00026	7375	17467	29888
11	0,00039	4844	11472	19629
12	0,00058	3300	7815	13373
13	0,00082	2318	5490	9395
14	0,00114	1672	3960	**6775**
15	0,00154	1233	**2921**	4997
16	0,00205	928	**2197**	3759

17	0,00268	710	1682	2877
18	0,00344	552	1307	2236
19	0,00437	435	1030	1762
20	0,00548	347	821	1405
21	0,00680	280	662	1133
22	0,00835	228	539	923
23	0,01015	187	443	758
24	0,01225	155	367	629
25	0,01467	130	307	525
26	0,01744	109	258	442
27	0,02059	92	219	374
28	0,02418	79	186	318
29	0,02823	67	159	273
30	0,03278	58	137	235

It has been reported that for a given age, a slower diffusion rate obsidian generally yields a more precise OHD age than a fast diffusion obsidian. This has been seen by examining the two "rate based on source" cases of Bodie Hills and Coso West Sugarloaf obsidians. With diffusion rates of 18.14 μ^2 /1000 yrs at EHT = 20°C for Coso against 10.38 μ^2/1000 years at 20°C for BH a great difference between these two different sources. The differences are due to chemical content, structural issues, water content, melting temperature during formation. The uncertainty for Coso is always greater than the corresponding uncertainty for BH, and the source rate method yields age coefficients of variation between approximately ~13% for Bodie Hills and ~26% for Coso West Sugarloaf. The hydration rate was then computed from the total wt% H2Ot. In fact, for two groups of BH source the hydration rate at 20oC for Group 1 is 11.25±0.83 μ2/1000 years and for Group 2 it is 10.0±0.43 μ2/1000 years; a composite rate for all samples is 10.36±0.72 μ2/1000 years (see Basgall 1990; Rogers and Yohe 2011; Rogers and Stevenson 2022b; Rogers 2013). The BH field source variation in water and density has been reported by Stevenson et al., (2023).

On the other hand, the calculated hydration rates per temperature for the aged experiments are in Table 4B.

It appears that the hydration rate of aged data for T=20oC BH is 11% lower than that of Group 1 and almost like Group 2. For Lower temperatures drastic change occurs. The Arrhenius plot of aged data for T=16-20oC gives for the 1.9micron sample ages ±19% around the known age, for the 4.5micron sample ±22% and for the 7.7-micron sample ±28%. However, for T=18oC the agreement is very close to the known ages.

The Gr of the two aged NV samples produced ages deviated -6%, +16% and -26% from the known ones without reference to EHT. Last, for the power law of BH applied to NV the ages were <1% different from the known ones for 12-14oC.

In our approach of microns/ microns.yr-1 the corresponding ages per sample that are close to the known ones occur for temperatures of 18-19oC, 15-16oC and ~14oC respectively, following a stratigraphic order of depth below ground.

Accelerated hydration of one sample from each group verified the hydration rate determinations from values of structural water content. These findings demonstrate that obsidian sources may vary in terms of obsidian structural water and display various rates of hydration. If not accounted for, misguided obsidian dates can be produced, resulting in inaccurate chronological conclusions. (Rogers & Stevenson 2023; Stevenson et al., 2023).

In any case the obtained ages for Porc Epic based on BH data verify our statement that in OHD one must have aged data for the source, and then computing a specimen-unique power law for a proper hydration rate which will greatly increase precision. In cases where the obsidian sources do not differ much in (California and Easter Islands) the larger age difference is 5-6% for young ages and about 20% for larger ages.

With our method of power law of the five experimental temperatures from Bodie Hills extrapolated to environmental T (as pixels/yr), in the NV samples the 1st sample of 472 years corresponds to 462 years and av. T 13oC; the 2nd sample 2646 years corresponds to 2600 years and av T 14oC; the 3rd sample =7747 yrs correspond to 7654 and average T oC=12oC.

Subject to the fact that these samples were found in a cave at different depths under surface where temperatures for the first meter lie between 12-16°C (California 2015 av. T =12°C) the obtained ages are very satisfactory corresponding to 12-14°C where the depth of the sample corresponds with the anticipated temperature which lowers by depth.

Comparing NV calculated ages with the those of eq.2 and Arrhenius plot for 18°C our results are very satisfactory and concordant to those and with the reported known data. Bearing in mind that the three samples were coming from different stratigraphy depth below ground the burial temperatures are bound to differ. In particular the 1.9 micron sample gave an age difference of 1 year between eq.2 and hydration rate based on water content approach and Arrhenius plot (Stevenson et al., 2023) and our approach of power law of BH for T=20°C (Table 6) i.e. the correlation between depth in microns/year and the temperature from the BH aged experiments (from Fig.7B), without normalization, using only data in microns of the thickness.

3.3.2 Ethiopean tentative ages

The African blades from Ethiopia, Porc Epic cave, Dire Dawa (Clark et al., 1984) produce tentative ages **firstly**, according to the power law and normalized pixels per year of the three known ages of NV data, **secondly** on BH pix/yr normalized to BH, and **thirdly** with growth rate. NV and BH data are from California and hence use in Ethiopean obsidian is very indicative but show the potential of using alternative methods if experimental data are available.

First, eq.8 is used of the power law of the three known ages NV (whereas A is the age and x the number of normalized pixels of eq.8) for estimating independently of other parameters the Ethiopian ages. The ages obtained are 19,383 years for PE-21 and 21,600 years BP for PE-23 (Table 7).

Table 7: African ages based on 3 NV power law for the (unknown) temperatures the 3 NV were subjected. Data on hydration rim in microns and respective pixels (1 pixel for present analysed images = 0.19 μm from 46.99/247 pixels measured by us)

Lab. No/Sample	Width	Height	Hydration layer Width (μm)	Total pixels norm to NV	Norm. to NV Hydration layer pixels	% hydrated	Age, years BP on 3 NV power law eq.11
Ethiopian Blades - PE-21 600x Exterior, RBC-581A	1429	1072	46.99~247 pixels	1,531,888	235,587	15,38	19,384
Ethiopian Blades - PE-23 600X Fissure, RBC-583A	1429	1072	43.71~ 230 pixels	1,531,888	261,367	17,06	21, 600

On the other hand, in second alternative the ages with power law of BH of T Versus pixels/yr, non-normalized (800*600 pixels image size for Ethiopian blades), vary between around 1,200 to 45,000 years BP. In same time BH images were normalized from 320*240 to 1429*1072 pixels image size of NV, too, and the ages ranged between 7,000-280,000 years on these normalized values to NV for temperatures 10-31°C (Table 8). For the latter for 15-17°C (most probable) the calculated ages are 46-69,000 years for PE-21 and 51-76,000 for PE23. One can realize here the compulsory normalization in such dating calculations. (see **APPENDIX Table A4** for the age difference between PE21 and PE23).

Table 8: African blades of normalized (to BH) hydration layers in pixels dated by BH power law data for temperatures 10-31°C. In red are environmental expected archaeological temperatures 10-16°C and respective calculated ages.

T based on BH power law	Pixel/60	Pixel/day	Pixel/year	PE21-AGE on BH power law data, eq.10 non norma.	PE23- AGE on BH power law data, eq.10 non-norm.	PE21 AGE norm. to same area of BH	PE23 age norm. to same area of BH
10	0,96	0,016	5,83	40426	44850	252661	280310
11	1,30	0,022	7,91	29790	33050	186187	206561
12	1,72	0,03	10,45	22544	25011	140898	156316
13	2,22	0,04	13,50	17445	19354	109032	120964
14	2,81	0,05	17,12	13759	15264	85993	95403
15	3,51	0,06	21,36	11031	12238	68942	76486
16	4,32	0,07	26,26	8971	9952	56066	62201
17	5,24	0,09	31,89	7387	8196	46170	51223
18	6,30	0,10	38,30	6151	6824	38446	42653

19	7,49	0,12	45,54	5173	5739	32332	35870
20	8,82	0,15	53,67	4389	4870	27433	30435
21	10,32	0,17	62,75	3754	4165	23464	26032
22	11,97	0,20	72,84	3235	3588	20216	22428
23	13,81	0,23	83,98	2805	3112	17533	19451
24	15,82	0,26	96,25	2448	2716	15298	16972
25	18,03	0,30	109,69	2148	2383	13423	14892
26	20,45	0,34	124,38	1894	2101	11838	13134
27	23,07	0,38	140,36	1678	1862	10490	11638
28	25,92	0,43	157,70	1494	1657	9337	10359
29	29,01	0,48	176,46	1335	1481	8344	9257
30	32,33	0,54	196,70	1198	1329	7486	8305
31	35,92	0,60	218,49	1078	1196	6739	7477

Third, making use of the Gr of the NV obsidians (the 3 and 5 averages from Table 4 in pixels/yr of three archaeological NV and the 2 aged ones), the ages calculated as pixels of Ethiopian samples (Table 8) ranged between about 17,000 years and 20,000 years BP.

For the **Gr growth rate**, we also use the ratio of (Hydration layer width in microns of the two Ethiopian samples, over, the microns per year from BH) for each temperature for the two samples and produce T versus age (Fig.10). This Gr alternative is using the BH temperature Versus microns/yr power law, eq.12, and the depth of the two Ethiopian samples and the ages computed are shown in Table 9 below which gives the age data for T=10-30 ^{o}C. From Table 10 and Fig.10 the ages are 31,000-57,000 years BP for T=13-15^{o}C.

Between 13-20 ^{o}C ages vary between 57,000 to 8,500 years BP and for 13-17^{o}C between 57,000 -17,000 years respectively.

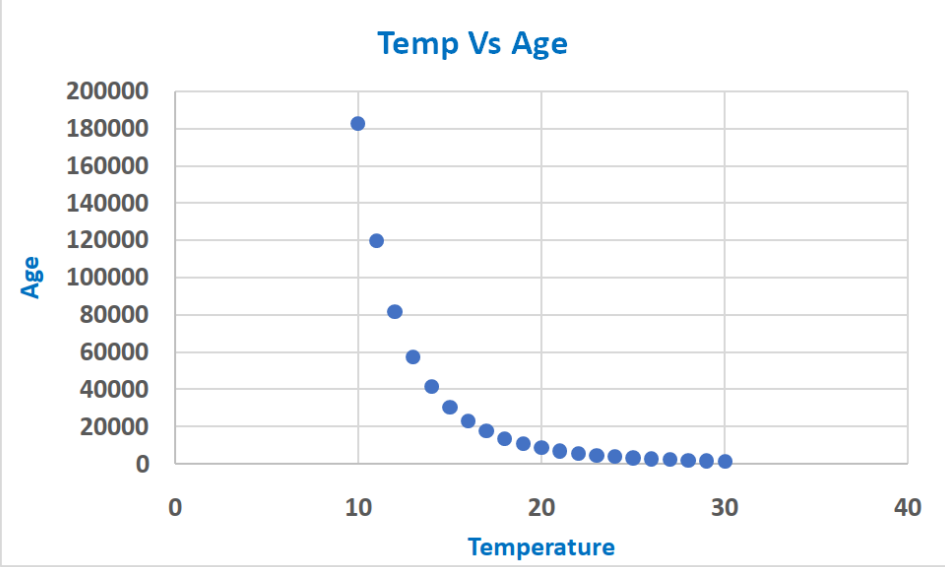

Figure 10: Temperature versus age for the PE-21 Ethiopean sample.

Table 9. A) Ages of the 2 Ethiopian blades and their ratio. Based on BH T Vs microns/yr power law, eq.12, the depth in microns from the Ethiopian samples the age is computed as Ethiopian hydration depth / hydration depth per year from BH. A difference of ca 7% as in their respective hydration thicknesses. Bold the most possible T. B) Ages per temperature based on hydration rates calculated from Arrhenius plot.

(A)

T°C	Age, years BP, PE-21 Microns/Microns.yr^{-1}	Age, years BP, PE-23 Microns/Microns.yr^{-1}	Ratio
10	182391,9	169660,5	1,07504
11	119790,5	111428,9	1,07504
12	81608,8	75912,33	1,07504
13	**57332,56**	**53330,63**	**1,07504**
14	**41346,11**	**38460,07**	**1,07504**
15	**30497,69**	**28368,88**	**1,07504**
16	22942,05	21340,65	1,07504
17	17558,82	16333,17	1,07504
18	13645,78	12693,28	1,07504
19	10750,37	9999,969	1,07504
20	8573,579	7975,125	1,07504
21	6913,471	6430,896	1,07504
22	5630,915	5237,866	1,07504
23	4628,326	4305,259	1,07504
24	3836,133	3568,363	1,07504
25	3203,997	2980,351	1,07504
26	2694,995	2506,879	1,07504
27	2281,707	2122,439	1,07504
28	1943,531	1807,868	1,07504
29	1664,822	1548,614	1,07504
30	1433,585	1333,518	1,07504

(B)

Sample/ T°C	20	18	16	14	12
PE-21	223131	284664	363920	470000	602000
PE-23	192986	246134	314662	406382	520435

The difference between PE-21 and PE-23 using BH temperature Versus depth in microns/microns.yr^{-1} power law is around 7% (See **APPENDIX Fig. A3**).

Applying the Arrhenius plot of BH data to Ethiopian gave ages extremely higher than expected from the stratigraphy of earlier reported sampling and dating at the cave site (>200,000 years or early middle stone age to late early stone age).

The temperature in the air outside is generally higher or more variable than the temperature inside a cave. It is known that in hot weather, caves are cooler than the air outside and in cold weather, caves may feel warmer than the outside air. This is why caves are often sought for shelter, especially in prehistoric societies, in extreme conditions, providing a naturally regulated temperature environment. At shallow depths, soil temperature is usually more stable than air, and air temperature can be higher or lower depending on external influences. At greater depths, soil temperature tends to be slightly higher than air temperature due to geothermal heat retention. Soil temperature varies with depth, but fluctuations decrease as depth increases, stabilizing at around 3-5 meters before geothermal heat becomes significant. These uncertainties reflect age approximation in our present cases.

It is known that across central Africa annual average air temperatures range from 24- 26°C and in soil is lower depending on the burial depth. But around the site Dari Dawa (Pork epic excavation) Ethiopia today average is 23oC in mean air temperature. In a cave the temperature could vary with depth and are less than open air temperature. Then the cave temperature gives the potential LSA age for these two blades

despite the power law of pixels area, eq.10, and temperature, which was based on the experimentally aged California obsidian (BH).

Clark et al., (1984) estimated the effective temperature to 24.8oC, based on an equation that depends on the mean annual air temperature; in turn their eq.2 gave 61-77,000 years. This is not correct because the aged experiments were not hydrated properly. The experiment by Joe Michels in this case study is seriously flawed in its design and should not be used. He used hydrating glass in 500ml of distilled water, which is a hydration-dissolution experiment. The hydration layer is forming but at the same time the surface is dissolving. This is why later scholars switched to vapor hydration many years ago.

As the authors noted, the effective temperature of the Pore Epic region is a very important part of the rate calculation. Thus, the glacial periods with subsequent lowering of temperature will, therefore, slow the rate of hydration. However, ages of about 40,000 BP up to 100,000 BP or more have been obtained for MSA occurrences from southern Africa and elsewhere (Singer and Wymer 1982).

Moreover, the burial depth, the stratigraphic integrity and the exact burial position of the present dated samples affect greatly any obtained result.

Estimating the temperature in caves in Ethiopia the 22-24oC range provide the ages obtained vary between 15-20Ka and 17-22 Ka BP for the PE21 and PE23 (Table 7) (such time range is quoted also by Phillipson 1982). It should be noted that both Middle Stone Age (MSA) and Late Stone Age (LSA) levels are extremely rare in Ethiopia, where most of the allegedly 'transitional' deposits have proved to be mixed or secondary contexts (Brandt 1986, 62; Fernández et al., 2007). Therefore, the obtained ages are tentative due to the abovementioned unknown factors.

DISCUSSION

BH is diverse source, and the aged experimental results have shown some inconsistency at 170°C. This may explain the attached errors in the power law fitting.

The long ascertained non-linear behavior of hydration thickness in the deducted OHD ages for environmental temperatures extrapolated from high temperature aged experiments (usually 120-200°C) have been considered. The prompt use of a power law derives from the empirical OHD age equation and from the physics and chemistry of the diffusion process which suggest that the relationship between age and rim thickness should be approximately quadratic.

The African ages obtained based on Californian obsidian (power law of NV and growth rate) are for PE-21, 17-19,000 years and for PE-23 lie between 19-21000 years BP. Obviously the quite different obsidian sources have different hydration rates and until more data on the Ethiopean samples are available the present attempt is indicative. However, the BH power law of pixels/yr for temperatures 15-17°C provide MSA ages (ca 41-69 Ka and ca.51-76 Ka) respectively for PE21 and PE23.

The African samples come from what was thought of as a Middle Stone age. However, excavation in 1974 revealed that the Middle Stone Age levels had been trapped behind a giant dripstone, except for the front half of the cave, where weathering and later deposition had caused the apparent mingling of Middle and Later Stone Age objects noted by the 1933 excavators. The site is mostly made up of points, scrapers, and edge-damaged blades and flake forms. The sophisticated nature of the retouched and used implements, the cave's relative limited access and the crushed character of the bone debris, imply that the cave was probably used as a hunting camp during seasons when game moved into the escarpment adjacent to the Afar Plains.

The major MSA habitation was located inside a 1.5 m thick layer of indurated, coarsely laminated calcareous cave breccia that was placed over this. Late prehistoric occupation of the cave continued during the deposition of a 20–25 cm layer.

The fact that the MSA items were sealed and stratigraphically distinct everywhere else in the cave save at the entrance was therefore abundantly obvious from their excavated section. There, after dripstone cutting and filling, LSA and lingering MSA artifacts naturally mixed. The later Stone Age was discovered in the uppermost layer of fine sands and loam, and the 1933 excavation backfill also contained 27 potsherds and based on typology, a number of LSA objects.

Despite the dating efforts of charcoal by C-14 and stalagmite by U234/Th230 disequilibrium dating (with ages ranged between 4500 to 6800 years BP) it seemed that the age of the MSA occupation would remain unknown. Initial OHD provided a testing of the model presented, namely that Pore Epic was the fall and/or spring camp of an old group of MSA hunters' site.

Summarizing it is worth noting that the alternative ways to date obsidians based mainly on a power law in the diffusion rate and hydration growth are a considerable attempt within the current limitations in the dating errors. Despite distant sources the reasonable result is reinforced also from the fact that anhydrous chemistry has a negligible effect on hydration rate. Structural water, on the other hand, has a profound effect on obsidian hydration rate (Franchetti et al.,

2024; Stevenson et al., 2019a). This has been reported in earlier studies of glass materials.

The extent of hydration was observed to fluctuate in accordance with the concentration of Si-OH groups, which is significantly influenced by the presence of (1) modifier ions or non-bridging oxygen, (2) glass intermediates (such as Al_2O_3 or Fe_2O_3), and (3) water that is already encapsulated within the bulk structure of the glass. The physical adsorption of water (hydration) on multicomponent glass exhibits notable differences and increased complexity when compared to silica, owing to the structural discrepancies between the two materials. In the case of pure silica, the predominant sites available for physisorption on the surface are primarily constituted by silanol groups. Conversely, in multicomponent glasses, there exist additional active surface sites, including non-bridging oxygen or alkali ions, which facilitate the enhanced adsorption of molecular water. The molecular water has the capacity to interact with non-bridging oxygen, leading to the generation of free modifier ions and H-bonded silanol groups. The silanol groups demonstrate a high reactivity towards the adsorption of molecular water. Moreover silanols follow a similar depth profile manner as H^+ (Liritzis and Laskaris, 2009, 2011), implying it following same reaction process as hydrogen. Moreover, multicomponent glasses allow a higher degree of hydration, (e.g. hydrated not only at the surface but also in the bulk (near-surface)) in contrast to pure silica surfaces where the formation of silanol groups is usually limited to a monolayer on the surface (Ito and Tomozawa, 1982; Scholze 1966; Zhuravlev 2000).

Other sources of error present in OHD in general are also the relative humidity, geochemistry, the heterogenic disorder and fragmentation, capacity of percolation (Liritzis et al., 2024) form a multiparametric complex phenomenon. If one isolates one of them which influences hydration rate, it does not give the real status of diffusion rate. While the high temperature experiments, the hydration depth, and growth rates characterize the final effect of all parameters involved in the diffusion process. Hence, our alternative approaches as based on the cumulative effects of all parameters, they are bound to provide a more reliable date. It has been proposed that during water diffusion within the bulk glass that molecular water (H_2Om) moves through the glass in a series of jumps into "doorways" or small interstitial sites (Doremus 2002). The rate at which this process occurs depends upon the intermolecular distance of the host material matrix compared to the size of the diffusing species (Liritzis 2006). There is also a conversion between H_2Om and OH which occurs at these higher temperatures, but this reaction is temperature dependent, and greatly reduced to below 400^{o}C (Nowak and Behrens 1995) and inferred not to be detectable in obsidian hydrated at ambient temperature. (Anovitz et al. 2008). Hence, the light passing through the hydration layer which reflects to respective pixels density may be related to internal stress created by more OH conversion at higher temperature which could impact transmittance. The light absorption coefficient of water is dependent on temperature and concentration of ions, i.e. the salinity in seawater, hydroxyls etc. (Röttgers et al., 2014; light absorption at a specific wavelength change linearly with temperature (Collins 1925; Sullivan et al., 2006). In principal density changes with temperature do change the pure water absorption coefficient. When density decreases the number of molecules per volume or optical path decreases (Zhang and Hu, 2009).

The dominant vibrational features of the two O-H bonds leading to major absorption maxima are symmetric and asymmetric, stretching, and bending of the molecule with wavenumbers (wavelength). In the liquid state rotations of the molecule are not free (leading to many rotational-vibrational combinations and millions of absorption lines) but are limited by hydrogen bonding in the water molecule cluster and are reduced to three so-called libration modes that have weaker influences than the vibrations and are, hence, at lower wavenumbers. Accurate knowledge of the water absorption/transparence coefficient, and/or its temperature correction coefficients, is essential for a wide range of optical applications. Therefore, temperature has an impact of optical density (and refractive index) which if fitted to a range of extrapolated temperatures seems to provide a good modelling of optical density expressed by pixels quantity in the hydration layer.

We have elaborated on the above and have shown that pixels could be related to temperature, maybe using water pixel intensity. The amount of light passing through the hydration layer has been correlated to temperature. The total pixels in the hydration layer versus temperature has been shown in Fig.5A. By preprocessing original image using the Mode threshold the binarization images of the five BH aged experiments were obtained (see for example the black pixels in Fig.5D). The light pixels which represent potential water as described by fractal dimensions in the hydrated and non-hydrated parts of archaeological obsidians (see Liritzis et al., 2024) within the hydration belts in Fig.5C were binarized to black pixels.

Moreover, the power law has been found in water pixels (black pixels from Fig.5D) versus temperature (Fig.11 A, B) with a relevant similar exponent about 3.2 (Fig.7A, B) like in total pixels plot in rim (and without water pixels). The related equation becomes:

$$A=0.0002*T^{3.26},\ R^2=0.97 \quad (13)$$

where A the area in water pixels/year and T the temperature.

In Fig.11C it is striking the high correlation between water pixels and total pixels in the hydration layer with a $R^2=1$. This implies that one may use total pixels with temperature power law for dating purposes. This has been also validated by the agent of depth in microns correlated by total pixels.

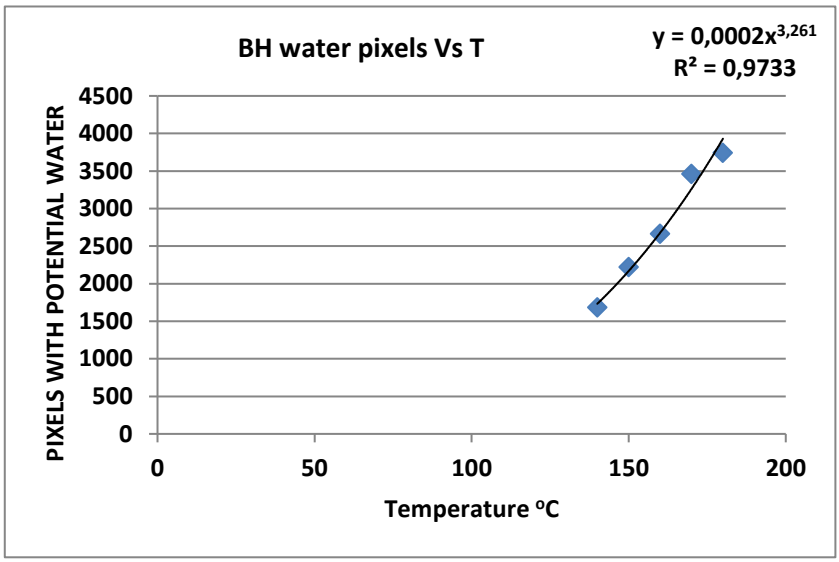

(A)

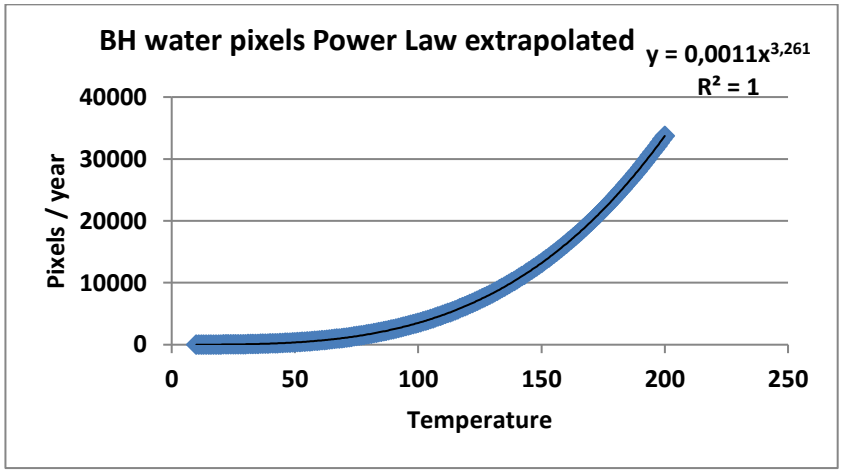

(B)

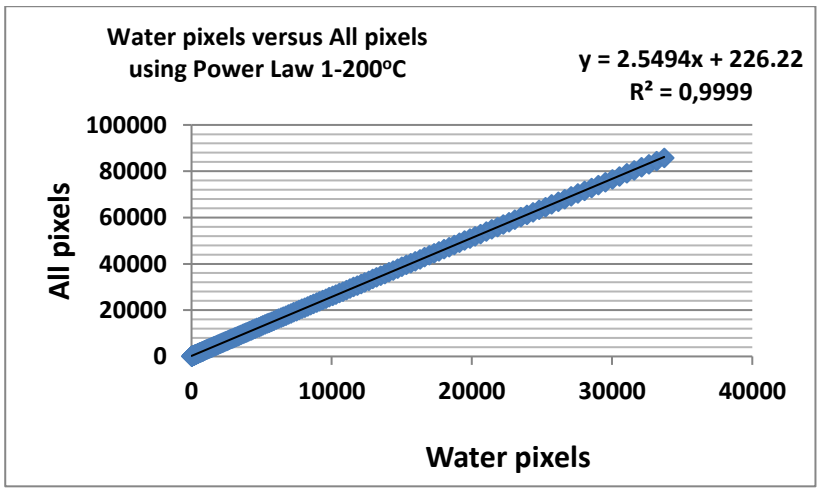

(C)

Figure 11. A) fitting the five points by a power law function, B) Power law extrapolated to ambient temperatures, and C) correlation between total pixels and water pixels.

It should be pointed out that the ratio of water pixels -to -depth is not particularly accurate due to the errors involved in the determination of the boundaries of the front diffusion and the tail at the end of hydration layer. But the result of the power law extrapolation smooths out these differences that may occur at high T.

Last, according to Mazer et al. (1991), using optical microscopy, the hydration rate increased by about x1.2 times between 90% and 100% relative humidity, but was not significantly affected by relative humidity below 80%.

The calculated NV ages from the BH power law and growth rate of experimentally aged data provide ages within 6-20% of the calculated earlier by OHD, which is a remarkable result.

The determination of power law exponents has already been proposed to create universality categories that consider the dimensionality and type of perturbation present in a diffusive environment. Thus, the power law can be used in diffusion in solids problems. Here we use it as an alternative dating process to the conventional Arrhenius and Friedman & Smith empirical equation. Though from five BH the A and E from rim and for certain T may produce a k, a comparison of ages of present approaches and earlier methods seem of interest and our approach is validated.

Here we are dealing with several experiments on obsidians of various sources, though more geographically dispersed are needed for future work. It appears that the power law applies to all of them either as pixels or pixels/year, microns/year and ages versus pixels. The overall dating error of these different obsidian sources lies between 7-20% depending on the accuracy of used data. Thus, the present approach is a bit faster, versatile and of better precision for accuracies ranging like those of older methods (if not better). In the Ethiopian case the age deviations between conventional method with the Arrhenius plot and the present alternatives are high.

Power law is applied to four different glasses of different water content, and it appears that the high temperature data extrapolated to environmental burial temperatures compensate for the past variable agents of the obsidian body. It seems that the power law in different obsidians have a different exponent but relatively similar behavior in age calculation. Hence the power law is sensitive because the method was applied to a variety of accelerated hydration experiments of different obsidian composition and the exponent varied to reflect the rate differences, thus we obtained satisfactory results. That is close to expected NV ages and reasonable ones for Ethiopian. In fact, the power law exponents are 3.2 for BH T versus pixels, 4.4 for BH T versus microns and 1.04 for ages versus pixels.

The difference between the pixels and depth approaches is possibly due to the different input data and / or to the fact that micron analysis is based on a direct, primary determination and does not consider the image size, and pixel analysis were used on possibly not original images. Also, the differences may reflect structural status in obsidians. More accurately here is the power law of T versus microns because we know the exact value of hydration depth. In future we expect these exponents and associated coefficients of power law equation to have a corresponding value depending on the obsidians measured.

The test cases are diverted with regards to sources, older experiments, different operators and some absolute dating weakness. The present alternative dating is a pioneering attempt for further development using more consistent samples of controlled dates. Porc Epic samples are not directly associated with the radiocarbon dates and stratigraphy problematic; thus, our proposed ages are tentative but fall within the expected archaeological phases of the site.

At any rate, for the safer power law equation samples for dating and aged experiments must be of similar source or other characteristics of structure. Also, for uncalibrated areas rescaling to known images is required.

Failing to maintain these requirements an erroneous age result is expected. An example comes from the reported data for Shirataki (Japan) of 4.5μm rim and ca 8oC temperature (Nakazawa 2016). The expected OHD and C-14 date is ca 18,000±1000 years and with our approach gives ca 27,000 years BP (though the reported EHT is not reliably estimated based on last century data for a late glacial and interglacial burial period of the sample).

Overall, the three alternative approaches devised and proposed with prominent power law dependence of temperature versus hydration area in pixels per duration of aging or microns, seem to open new directions in OHD and offer a means of dating ancient obsidian tools. (see **APPENDIX Steps to obtain a date**).

The high temperature experiments made in the past to accommodate data in the Arrhenius plot and estimate the diffusion rate at ambient (burial) temperatures, calculated by a formula, seem to provide accurate pixels of hydrated area per reasonable estimated environmental temperature values due to power law dependence.

The limitations of the power law dating (beyond similar obsidian sources) on pixels image data lie in the manner of taking images by microscopes their magnification and resolution (e.g. the Becke lines at

both the rim/mounting medium causing the hydrated/unhydrated glass boundary to be gradational, not sharp, Anovitz et al., 1999), hence normalization which is always recommended. More data is required to investigate the power law exponents. At any rate even though the hydration depth is the basic parameter to OHD is capable but not sufficient for the study of diffusion and the determination of age. The SIMS H+ profiling as well the fractal valuation of hydration layer have demonstrated the need for an additional agent to account for submicron variations in the hydration layer flow. Hence any new OHD development may or may not turn back to older methods and it is a worthy attempt.

CONCLUSION

The produced thin sections, experimentally induced hydration, the image processing methodology and analysis are academically sound and properly placed in the frame of current and past research. We have provided appropriate evidence and reasoning for the conclusions made regarding the use of the diffused layer developed per aged experiments at high temperatures in obsidian artifacts.

A model is proposed and a power law formula to convert image data (pixels and thickness) to ages. The known temperature dependence of hydration can be approximated from available soil effective temperature data and hence the OHD can be achieved through three ways. From the power law of Temperature versus hydration layer pixels area, the growth rate of the hydration layer per temperature, from power law of known OHD ages and their hydration layer pixels and from power law of T versus the thickness in microns/year.

The three obsidian sources (and artifacts) were approached by the following methods. For the Orito (Easter Islands) the study the hydration layer was based on BH temperature power law at 160oC and compared to aged Growth rate; for Napa Valley the dating was based on the growth rate of experimentally aged NV samples, on the BH power law of temperatures versus area pixels, and on the power law of depth/year and the temperature without normalization. The Ethiopean dating was based on the three NV ages as power law and normalized pixels per year, on the BH power law (pixels/yr) normalized to BH and for different temperatures, on the growth rate of NV applied to Ethiopian, and on the power law of BH of Temperature versus the depth (microns/yr).

The power law of microns versus temperature is preferred to power law of pixels versus T because does not import image sizes and hence no normalization is required. The growth rates on the other hand do not include a functional dependence but only a ratio which is the function of time. In the initial diffusion the rate is not of the same order as in longer times explained by the quadratic dependence of diffusion with time and the power law found here. Moreover, the close to surface saturation layer provides a virtually new start of diffusion that eventually makes the variation of water follow two mechanisms, one based on Fick's law and another exponential like that tends to zero at the hydration tail.

This novel research makes a significant contribution to the academic field of the diffused obsidian and its hydration dating. More geographically and compositionally diversified obsidian sources are needed to verify and clarify the power law relationship, and this is the goal of our next work.

Authors contribution: Conceptualizing: I.L.; methodology, I.L., I.A.; software, I.A., I.L.; validation, I.L., I.A.; formal analysis, I.L., I.A.; investigation, I.L., I.A.; resources; data curation, I.A., I.L.; writing—original draft preparation, I.L.; writing—review and editing, I.L., I.A.; visualization, I.L., I.A.; supervision, I.L.; project administration, I.L. All authors have read and agreed to the published version of the manuscript.

Acknowledgements: We are thankful to Chris M Stevenson for his support with data provision and discussion and constructive comments on the manuscript, Dr A.Rogers for useful data on temperature, Dr Tom Origer& Associates, for data provision and reading the manuscript and Dr Nikos Laskaris for constructive comments.

APPENDIX

Activation Energy, E

The activation energy, E, in the context of chemical reactions, represents the minimum energy required for reactants to reach the transition state and form products. It is usually expressed in joules per mole (or kilojoules/mole). Whether E is dependent on a source or burial environment depends on the context of the reaction or process being studied. Let's clarify:

Source or Burial Environment Effects on E:

1. Chemical Reaction Characteristics:

• **Intrinsic Property**: The activation energy is an intrinsic property of a chemical reaction and depends on the specific reactants, products, and reaction pathway. This means E does not inherently depend on external conditions like the source or burial environment unless those conditions alter the reaction dynamics.

1. **Temperature and Pressure Influence**:

• Environmental factors such as temperature and pressure, which vary in source or burial environments, can influence the rate constant of the reaction through the Arrhenius equation (4). While E is considered constant for a given reaction, changes in temperature (common in burial environments) can indirectly affect observed reaction rates.

3. Physical and Chemical Changes in the Environment:

In burial environments, diagenetic changes (e.g., mineralization, organic matter transformation) might alter the reactants or reaction pathways, effectively leading to a new E.
Catalysts, present in certain source environments, can lower effective activation energy by providing an alternative reaction pathway.

4. Environmental History:

Source or burial environments can determine the composition of reactants (e.g., organic molecules in sedimentary basins), affecting which reactions are possible and their associated activation energies.

Conclusion:

E itself is not directly a constant of a source or burial environment but is tied to the specific reaction and its pathway. However, the environment influences the reaction conditions, and potentially the effective E by altering pathways or providing catalysts.

Segmentation and binarization protocol using ImageJ 1.54 open source based on java software

Step 1: Image Import
1. Open ImageJ.
2. Navigate to File > Open... and import the target image(s).
3. Ensure the images are compatible with ImageJ (e.g., .tif for high-resolution analysis).

Step 2: Apply a LUT
1. To enhance visualization, convert the image to a Look-Up Table (LUT):
- Go to Image > Lookup Tables > Select LUT... and choose the appropriate LUT (e.g., "Grayscale" or "Fire").
2. If needed, simplify the image by converting it to 8-bit:
- Go to Image > Type > 8-bit.

Step 3: Manual Segmentation of the Hydration Belt
1. Use the Freehand Selection Tool in the toolbar to outline the boundaries of the hydration belt manually.
2. Adjust the selection as needed:
- Use Edit > Selection > Enlarge... or Contract... to fine-tune the boundary.
3. Save the selection:
- Go to Edit > Selection > Save Selection... to retain a reusable version of the boundary.

Step 4: Create a Binary Mask
1. Convert the selected boundary to a binary mask:
- Navigate to Edit > Selection > Create Mask.
- This creates a binary image with the hydration belt as the white region and the rest as black.
2. Refine the mask:
- Use Process > Binary > Erode or Dilate to improve edge definition.
- Optionally, fill gaps within the mask using Edit > Fill.

Step 5: Extract the Hydration Belt from the Original Image
1. Combine the mask with the original image:
- Go to Process > Image Calculator..., select the original image and mask, and apply the operation AND or Multiply.
2. Save the resulting image, which isolates the hydration belt.

Step 6: Rotate the Segmented Hydration Belt

1. Rotate the extracted hydration belt:
 - Go to Image > Transform > Rotate..., and input the desired rotation angle.
2. Save the rotated image:
 - Use File > Save As... to preserve the rotated output.

Step 7: Binarize the Rotated Hydration Belt

1. Convert the rotated image to a binary format:
 - Go to Image > Adjust > Threshold... and adjust the slider until the hydration belt is clearly segmented.
2. Apply the threshold:
 - Click Apply to finalize the binary transformation.
 - The hydration belt will now appear as a black-and-white binary image (white for the belt, black for the background).

(Schindelin et al., 2015; Schneider et al., 2012)

Hydration layer dependence on Temperature of Bodie Hills

The three equations of the five temperatures versus hydration layers in pixels are given in Figure A1.

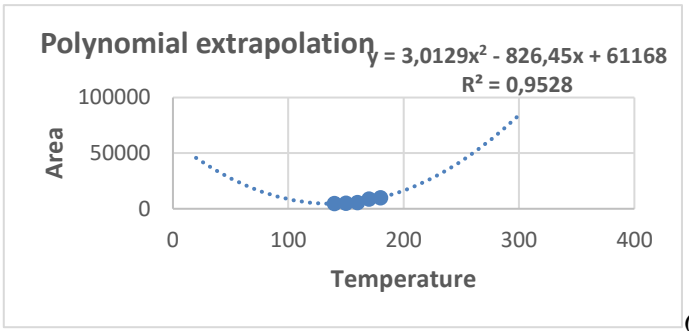

(A)

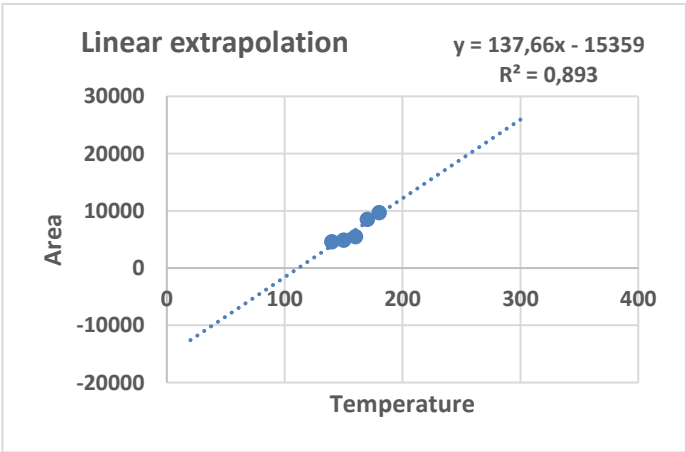

(B)

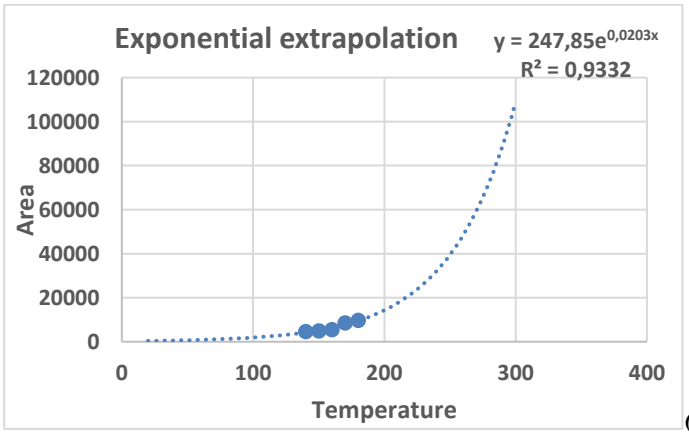

(C)

Figure A1. Fitting function of the 5 temperatures of BH1 by a) polynomial, b) linear, and c) exponential laws, with extrapolated (dashed) points.

Table A1: The power law of BH1 five temperatures hydration rim versus pixels extrapolated from 10 to 300 oC. In red the used data.

Temp.oC	Power Law with 5 points
20	8
30	30
40	76
50	155
60	277
70	454
80	697
90	1016
100	1424
110	1932
120	2553
130	3299
140	**4637**
150	**4926**
160	**5528**
170	**8520**
180	**9723**
190	11122
200	13107
210	15323
220	17785
230	20506
240	23500
250	26781
260	30365
270	34266
280	38498
290	43077
300	48017

A summary of all obsidians studied hydration belts is given in Fig.A2 and Table A2.

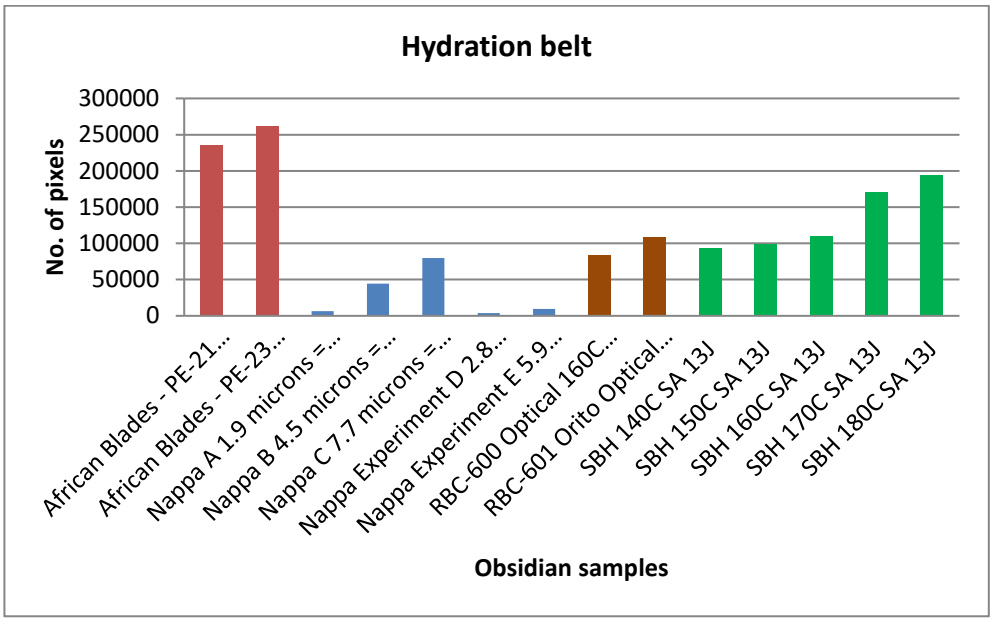

Figure A2 Normalized hydration layers of 1429x1072 Napa Valley image.

*Table A2: Hydration layers and percentage of full images for the 14 samples. All images were rescaled to 1429*1072 according to Napa Valley images.*

Samples	width	height	Total	Hydratic belt	% hydratic belt from full images
African Blades - PE-21 600x Exterior	1429	1072	1531888	235587	15,37887
African Blades - PE-23 600X Fissure	1429	1072	1531888	261367	17,06176
Napa A 1.9 microns = 472 years	1429	1072	1531888	6243	0,407536
Napa B 4.5 microns = 2,646 years	1429	1072	1531888	44448	2,901518
Napa C 7.7 microns = 7,747 years	1429	1072	1531888	79989	5,221596
Napa Experiment D 2.8 micron = 150 10	1429	1072	1531888	3989	0,260398
Napa Experiment E 5.9 micron = 140 60	1429	1072	1531888	9409	0,614209
RBC-600 Optical 160C 30 day	1429	1072	1531888	83745	5,466783
RBC-601 Orito Optical 160C 50 day 2	1429	1072	1531888	108758	7,099605
SBH 140C SA 13J	1429	1072	1531888	92518	6,039475
SBH 150C SA 13J	1429	1072	1531888	98330	6,418877
SBH 160C SA 13J	1429	1072	1531888	110209	7,194325
SBH 170C SA 13J	1429	1072	1531888	169952	11,09428
SBH 180C SA 13J	1429	1072	1531888	193866	12,65536

Different obsidians (sources) hydrate with different growth rates in natural hydration or experimentally lab- induced hydration.

Growth rates of BH are given in Table A3.

Table A3. Bodie Hills BH1 Growth Rates.

	Total pixels	Hydratic belts	%	Growth rate	
BH 140C A 13J	76800	4637	6,03776		
BH 150C A 13J	76800	4926	6,414063	1,062325	1,062325
BH 160C A 13J	76800	5528	7,197917	1,19215	1,122209
BH 170C A 13J	76800	8520	11,09375	1,837395	1,541245
BH 180C A 13J	76800	9723	12,66016	2,09683	1,141197
				1,547175	

Regarding the OHD in the set of aged Napa Valley images we use the hydration band measurements with bands developed on an obsidian source (Napa Valley in northern California) for which a hydration rate was previously calculated from associations with obsidian specimens and features that had been radiocarbon dated. Our experience has shown that hydration rates can be calculated from the comparison of hydration band measurements of an unknown source with the known source (Napa Valley). To add to the complexity of the study of hydration, lab created hydration has shown that some geochemically identified obsidian sources have multiple hydration rates, but standard XRF analyses cannot sort them.
The difference in the ages of PE-21 and PE-23 the 2 African blades based on the power law of BH1 T versus microns/microns.yr^{-1}, a difference of ca 7% as in their respective hydration thicknesses is shown in APPENDIX Fig. A3.

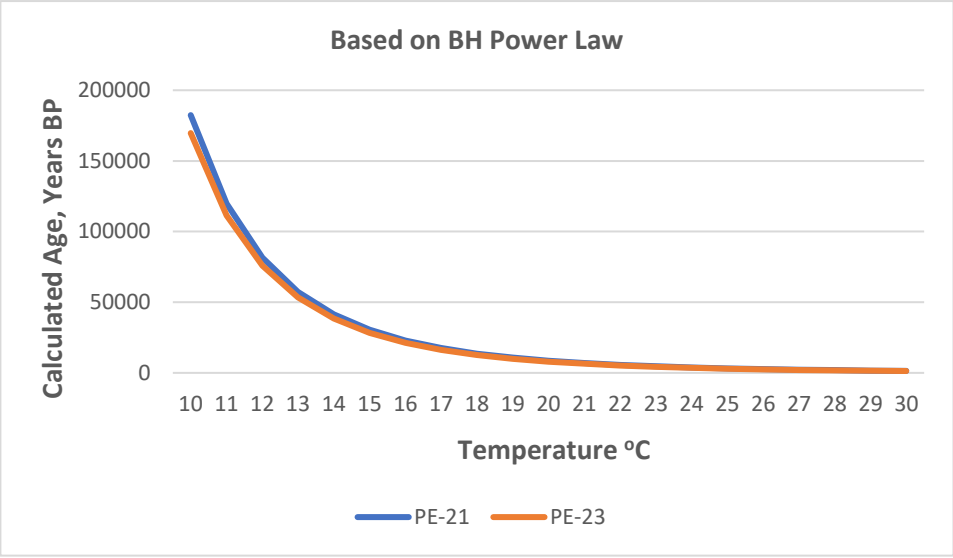

Figure A3: Difference in the ages of PE-21 and PE-23 2 based on the power law of BH1 T versus years.

Table A4. A) Ages of the 2 Ethiopian blades and their ratio. Based on BH1 T Vs microns/yr power law, the depth in microns from the Ethiopian samples the age is computed as Ethiopian hydration depth/ hydration depth per year from BH. A difference of ca 7% as in their respective hydration thicknesses. B) Ages per temperature based on hydration rates calculated from Arrhenius plot.

(A)

T°C	**Age, years BP, PE-21 Microns/Microns.yr^{-1}**	**Age, years BP, PE-23 Microns/Microns.yr^{-1}**	**Ratio**
10	182391	169660	1,07504
11	119790	111428	1,07504
12	81608	75912	1,07504
13	**57332**	**53330**	**1,07504**
14	**41346**	**38460**	**1,07504**
15	**30497**	**28368**	**1,07504**
16	22942	21340	1,07504
17	17558	16333	1,07504
18	13645	12693	1,07504
19	10750	9999	1,07504
20	8573	7975	1,07504
21	6913	6430	1,07504
22	5630	5237	1,07504
23	4628	4305	1,07504
24	3836	3568	1,07504
25	3203	2980	1,07504
26	2694	2506	1,07504
27	2281	2122	1,07504
28	1943	1807	1,07504
29	1664	1548	1,07504
30	1433	1333	1,07504

(B)

Sample/ T°C	**20**	**18**	**16**	**14**	**12**
PE-21	223131	284664	363920	470000	602000
PE-23	192986	246134	314662	406382	520435

Steps to obtain a date

Uncalibrated images (not in scale)

1.In a thin sectioned image of dated sample apply protocol of segmentation and binarization and measure **the number of pixels** of the rectangular hydration belt.

2. Similarly measure the **number of pixels /duration** (transform to per year) of experiments of hydration areas of the aged experiments at high T (e.g. 140, 150, 160, 170, etc). A)If the source of the sample is known from chemical analysis then the ageing is applied to similar source sample from lab induced experiments or published images of same source. B) If the provenance is unknown then one relies on available published data of othrer sources like in present article.

If the resolution of the uncalibrated images are diferent the images (pixels /duration) will be rescaled according to the high resolution images, like in our article all images were rescaled to 1429*1072 according to Napa Valley images or the BH for Orito.

3. Apply Power Law like equation (10) from Step 2A extrapolating to lower T. If Step 2B is used then present BH experimental data can be employed to estimate hydration age (eq.10, Fig.7A).

Calibrated Images (scaled to microns)

1.In a thin sectioned image of dated sample measure the rim in microns (Fig.4)

2. Similarly measure the number of rims in microns /duration (transform to per year) of experiments of hydration areas of the aged experiments at high T (e.g. 140, 150, 160, 170, etc). A)If the source of the sample is known from chemical analysis then the ageing is applied to similar source sample from lab induced experiments or published images of same source. B) If the provenance is unknown then one relies on available published data of other sources like in present article. (the resolution is not necessary because these are scaled data)
3. Apply Power Law of equation (12) from Step 2A extrapolating to lower T. If Step 2B is used then present BH experimental data can be employed to estimate hydration age (Fig.7B, eq.12).

Growth Rates
1. In a thin sectioned image of dated sample measure the rim in microns or pixels (Fig.4, Fig.6)
2.From Step 2 above: Estimate the total (normalised) pixels or microns/time of aged hydration layer.
Growth rate (pixels/year or microns/time) per temperature for hydration duration t1 as ratios of pixels/time. In hydration belts for uncalibrated images the growth rates must be normalized. In our case the original size of images is rescaled (in our case BH images 320*240 (76800 pixels to the size of 1429*1072 Napa Valley).
Then calculate age from step 1 (pixels or microns) divided by step 2 (pixels/time or microns/time).

REFERENCES

Anovitz, L.M., Cole, D.R., Fayek, M. (2008) Mechanisms of rhyolitic glass hydration below the glass transition. *American Mineralogist*, Vol.93, 1166–1178, doi: 10.2138/am.2008.2516.

Anovitz, L.M., Elam, J.M., Riciputi, L.R., Cole, D.R. (1999) The Failure of Obsidian Hydration Dating: Sources, Implications, and New Directions. *Journal of Archaeological Science*, Vol.26, No.7, 735–752, doi: 10.1006/jasc.1998.0342.

Anovitz, L.M., Elam, J.M., Riciputi, L.R., Cole, D.R. (2004) Isothermal Time-Series Determination of the Rate of Diffusion of Water in Pachuca Obsidian. *Archaeometry*, Vol.46, 301–326, doi: 10.1111/j.1475-4754.2004.00159.x.

Anovitz, L.M., Riciputi, L.R., Cole, D.R., Gruszkiewicz, M.S., Michael Elam, J. (2006) The effect of changes in relative humidity on the hydration rate of Pachuca obsidian. *Journal of Non-Crystalline Solids*, Vol.352, 5652–5662, doi: 10.1016/j.jnoncrysol.2006.08.044.

Basgall, M.E. (1990) Hydration Dating of Coso Obsidian: Problems and Prospects. Presented at the Twenty-fourth Annual Meeting of the Society for California Archaeology, Foster City.

Basgall, M., and Giambastiani, M (1995) Prehistoric Use of a Marginal Environment: Continuity and Change in Occupation of the Volcanic Tablelands, Inyo and Mono Counties, California. Center for Archaeological Research at Davis, California.

Bettinger, R.L., Delacorte, M.G., Jackson, R.J. (1984) Visual sourcing of central eastern California obsidians. In: Hughes, R.E. (ed.) *Obsidian Studies in the Great Basin*, *Contributions of the Archaeological Research Facility*, University of California, Berkeley, pp. 63–78.

Brandt, S.A. 1986. The Upper Pleistocene and Early Holocene Prehistory of the Horn of Africa. *The African Archaeological Review* 4, 41–82

Clark, J.D., Williamson, K.D., Michels, J.W., Marean, C.A. (1984) A Middle Stone Age occupation site at Porc Epic Cave, Dire Dawa (east-central Ethiopia). *African Archaeological Review*, Vol.2, No.1, 37–71, doi: 10.1007/BF01117225.

Collins, J.R. (1925) Change in the Infra-Red Absorption Spectrum of Water with Temperature. *Physical Review,* Vol.26, No.6, 771–779, doi: 10.1103/PhysRev.26.771.

Crank, J. (1975) The Mathematics of Diffusion, 2nd ed., Clarendon Press, Oxford.

Doremus, R.H. (1969) The diffusion of water in fused silica. In: J.W. Mitchell (Ed.), *Reactivity of Solids*, Wiley, New York, pp. 667–673.

Doremus, R.H. (2000) Diffusion of water in rhyolite glass: diffusion–reaction model. *Journal of Non-Crystalline Solids,* Vol.261, 101–107, doi: 10.1016/S0022-3093(99)00604-3.

Doremus, R. H. (1994) Glass Science, 2nd. ed.Wiley Interscience, New York.

Doremus, R.H. (2002) *Diffusion of Reactive Molecules in Solids and Melts.* Wiley, New York.

Ebert, W. L., Hofburg, R. F., and Bates, J. K., 1991. The sorption of water on obsidian and a nuclear waste glass. *Physics and Chemistry of Glasses*, 32(4), 133–137.

Fernández, V.M., De La Torre, I., Luque, L., González-Ruibal, A., López-Sáez, J.A. (2007) A Late Stone Age sequence from West Ethiopia: the sites of K'aaba and Bel K'urk'uma (Assosa, Benishangul-Gumuz Regional State). *Journal of African Archaeology*, Vol.5, No.1, 91–126, doi: 10.3213/1612-1651-10087.

Franchetti, F., Neme, G., Gil, A., Salgan, M.L., Rogers, A.K., Davenport, J., Garvey, R., Trofimova, O., Ladefoged, T.N., Stevenson, C.M. (2024) Obsidian hydration dating by infrared transmission spectroscopy. *Archaeometry*, Vol.66, No.5, 949–966, doi: 10.1111/arcm.12982.

Friedman, I., Long, W. (1976) Hydration Rate of Obsidian: New experimental techniques allow more precise dating of archeological and geological sites containing obsidian. *Science*, Vol.191, No.4225, 347–352, doi: 10.1126/science.191.4225.347.

Friedman, I., Smith, R.L. (1960) A new dating method using obsidian: Part I, The development of the method. *American Antiquity*, Vol.25, No.4, 476–493, doi: 10.2307/276634.

Hall, M.G., Ingo, C. (2021) Half Way There: Theoretical Considerations for Power Laws and Sticks in Diffusion MRI for Tissue Microstructure. *Mathematics*, Vol.9, No.16, 1871, doi: 10.3390/math9161871.

Hughes, R.E. (1984) *Obsidian Studies in the Great Basin*. Contributions of the Archaeological Research Facility, University of California, Berkeley.

Ito, S., Tomozawa, M. (1982) Dynamic fatigue and water in glass. *Journal de Physique Colloques*, Vol.61, 823.

Karato, S. (2013) Rheological Properties of Minerals and Rocks. In: Karato, S. (Ed.*), Physics and Chemistry of the Deep Earth*, Wiley, pp. 94–144, doi: 10.1002/9781118529492.ch4.

Laskaris, N., Liritzis, I. (2020) Surface and interface investigation of archaeological obsidian artefacts with TOF-SIMS: case study. *Scientific Culture*. doi: 10.5281/ZENODO.4007733.

Lee, H.-H., Papaioannou, A., Novikov, D.S., Fieremans, E. (2020) In vivo observation and biophysical interpretation of time-dependent diffusion in human cortical gray matter. *NeuroImage*, Vol.222, 117054, doi: 10.1016/j.neuroimage.2020.117054.

Liritzis, I. (2006) SIMS-SS A new obsidian hydration dating method: analysis and theoretical principles. *Archaeometry*, Vol.48, No.3, 533–547, doi: 10.1111/j.1475-4754.2006.00271.x.

Liritzis, I. (2014) Obsidian Hydration Dating. In: Rink, W.J., Thompson, J. (Eds.), *Encyclopedia of Scientific Dating Methods*, Springer Netherlands, Dordrecht, pp. 1–23, doi: 10.1007/978-94-007-6326-5_39-1.

Liritzis, I., Andronache, I., Stevenson, C. (2024) A novel approach to documenting water diffusion in ancient obsidian artifacts via the complexity analysis of microscope images. *Journal of Archaeological Science,* Vol.161, 105896, doi: 10.1016/j.jas.2023.105896.

Liritzis, I., Diakostamatiou, M. (2002) Towards a new method of obsidian hydration dating with secondary ion mass spectrometry via a surface saturation layer approach. *Mediterranean Archaeology & Archaeometry*, Vol.2, No.1, 3–20.

Liritzis, I., Diakostamatiou, M., Stevenson, C.M., Novak, S.W., Abdelrehim, I. (2004) Dating of hydrated obsidian surfaces by SIMS-SS. *Journal of Radioanalytical and Nuclear Chemistry*, Vol.261, 51–60, doi: 10.1023/B:JRNC.0000030934.66579.54.

Liritzis.I, Stevenson.C, Novak.S, Abdelrehim.I, Perdikatsis.V and M. Bonini (2007) New prospects in obsidian hydration dating: An integrated approach. Proceedings of the Hellenic Archaeometry Society, Athens, *British Archaeological Reports (BAR) International Series*, 9-22.(\

Liritzis.I, Bonini.M and Laskaris.N (2008) Obsidian hydration dating by SIMS-SS: surface suitability criteria from atomic force microscopy. *Surface & Interface Analysis*, 40, 458-463.

Liritzis, I., Laskaris, N. (2009) Advances in obsidian hydration dating by secondary ion mass spectrometry: World examples. *Nuclear Instruments and Methods in Physics Research Section B: Beam Interactions with Materials and Atoms*, Vol.267, 144–150, doi: 10.1016/j.nimb.2008.10.092.

Liritzis, I & Laskaris, N (2011) Fifty years of obsidian hydration dating in archaeology, *J. Non Crystalline Solids,* 357, 211-219.

Liritzis, I & Laskaris, N (2012) The SIMS-SS obsidian hydration dating Method. In Ioannis Liritzis and Christopher M. Stevenson (Editors) (2012) The Dating and Provenance of Natural and Manufactured Glasses; (The University of New Mexico Press), 26-45.

Liritzis, I., Laskaris, N. (2021) Archaeological obsidian hydration dating with secondary ion mass spectrometry: current status. *Mediterranean Archaeology and Archaeometry*, Vol. 21, No 3, pp. 51-67. https://doi.org/10.5281/ZENODO.5598229

Mazer, J.J., Stevenson, C.M., Ebert, W.L., Bates, J.K. (1991) The Experimental Hydration of Obsidian as a Function of Relative Humidity and Temperature. American Antiquity, Vol.56, 504–513, doi: 10.2307/280898.

Nakazawa, Y., (2016). The significance of obsidian hydration dating in assessing the integrity of Holocene midden, Hokkaido, northern Japan. *Quaternary International* 397, 474–483. https://doi.org/10.1016/j.quaint.2015.01.029

Novikov, D.S., Jensen, J.H., Helpern, J.A., Fieremans, E. (2014) Revealing mesoscopic structural universality with diffusion. *Proceedings of the National Academy of Sciences of the United States of America*, Vol.111, 5088–5093, doi: 10.1073/pnas.1316944111.

Nowak, M., Behrens, H. (1995) The speciation of water in haplogranitic glasses and melts determined by in situ near-infrared spectroscopy. *Geochimica et Cosmochimica Acta*, Vol.59, 3445–3450, doi: 10.1016/0016-7037(95)00237-T.

Pearson, J.L. (1995) *Prehistoric Occupation at Little Lake, Inyo County, California: A Definitive Chronology*. Unpublished MA Thesis, Department of Anthropology, California State University, Los Angeles.

Rogers, A.K. (2006) Induced hydration of obsidian: a simulation study of accuracy requirements. *Journal of Archaeological Science,* Vol. 33, No 12, 1696-1705

Rogers, A.K. (2007) Effective hydration temperature of obsidian: a diffusion theory analysis of time-dependent hydration rates. *Journal of Archaeological Science*, Vol.34, 656–665, doi: 10.1016/j.jas.2006.07.005.

Rogers, A.K. (2008a) Obsidian hydration dating: accuracy and resolution limitations imposed by intrinsic water variability. *Journal of Archaeological Science*, Vol.35, 2009–2016, doi: 10.1016/j.jas.2008.01.006.

Rogers, A.K. (2008b) Field data validation of an algorithm for computing obsidian effective hydration temperature. *Journal of Archaeological Science*, Vol.35, 441–447, doi: 10.1016/j.jas.2007.04.009.

Rogers, A.K. (2013) Flow-Specific Hydration Rates for Coso Obsidian, *Society for California Archaeology Proceedings*, Volume 27, 281-294.

Rogers, A.K., Stevenson, C.M. (2022a) An equation relating obsidian hydration rate to temperature and structural water content. *IAOS Bulletin*, 1–15.

Rogers, A.K., Stevenson, C.M. (2022b) A summary of obsidian hydration dating science and method for archaeologists. *Working Paper No. MS234A*.

Rogers, A.K., Stevenson, C.M. (2023) Obsidian Hydration Dating: Summary and Status of a Physics-Based Approach. *California Archaeology*, Vol.15, 219–242, doi: 10.1080/1947461X.2023.2240124.

Rogers, A.K., Stevenson, C.M. (2024) A speciation model for water in obsidian. *International Association for Obsidian Studies,* Vol.72, 9–19.

Rogers, A.K., Stevenson, C.M. (2017) Protocols for laboratory hydration of obsidian, and their effect on hydration rate accuracy: A Monte Carlo simulation study. *Journal of Archaeological Science: Reports*, Vol.16, 117–126, doi: 10.1016/j.jasrep.2017.09.014.

Rogers, A.K., Yohe II, R.M. (2011) An improved equation for Coso obsidian hydration dating, based on obsidian-radiocarbon association. *Proceedings of the Society for California Archaeology*, Vol. 25, 1–15. http://scahome.org/sca-publications/articles-of-the-sca-proceedings/.

Röttgers, R., McKee, D., Utschig, C. (2014) Temperature and salinity correction coefficients for light absorption by water in the visible to infrared spectral region. *Optics Express,* Vol.22, 25093, doi: 10.1364/OE.22.025093.

Schindelin, J., Rueden, C.T., Hiner, M.C., Eliceiri, K.W. (2015) The ImageJ ecosystem: An open platform for biomedical image analysis. *Molecular Reproduction and Development*, Vol.82, 518–529, doi: 10.1002/mrd.22489.

Schneider, C.A., Rasband, W.S., Eliceiri, K.W. (2012) NIH Image to ImageJ: 25 years of image analysis. *Nature Methods*, Vol.9, 671–675, doi: 10.1038/nmeth.2089.

Scholze, H. (1982) Chemical durability of glasses. *Journal of Non-Crystalline Solids,* Vol.52, 91–103, doi: 10.1016/0022-3093(82)90283-6.

Singer, R., Wymer, J. (1982) The Middle Stone Age at Klasies River Mouth in South Africa. *Doctoral Dissertation, Stellenbosch University,* Stellenbosch.

Smith, C.I., Chamberlain, A.T., Riley, M.S., Stringer, C., Collins, M.J. (2003) The thermal history of human fossils and the likelihood of successful DNA amplification. *Journal of Human Evolution*, Vol.45, 203–217, doi: 10.1016/S0047-2484(03)00106-4.

Stevenson, C.M., Abdelrehim, I.M., Novak, S.W. (2001) Infra-red photoacoustic and secondary ion mass spectrometry measurements of obsidian hydration rims. *Journal of Archaeological Science*, Vol.28, 109–115, doi: 10.1006/jasc.1999.0559.

Stevenson, C.M., Mazer, J.J., Scheetz, B.E. (1998) Archaeological obsidian studies: method and theory. In: Shackley, M.S. (Ed.), *Advances in Archaeological and Museum Science*, Vol.3. Plenum Press, New York, pp. 181–204.

Stevenson, C. M., M. Gottesman, and M.Macko (2000) Redefining the Working Assumptions for Obsidian Hydration Dating. *Journal of California and Great Basin Anthropology* 22(2): 223-236.

Stevenson, C.M., Novak, S.W. (2011) Obsidian hydration dating by infrared spectroscopy: method and calibration. *Journal of Archaeological Science*, Vol.38, 1716–1726, doi: 10.1016/j.jas.2011.03.003.

Stevenson, C.M., Rogers, A.K., Glascock, M.D. (2019a) Variability in obsidian structural water content and its importance in the hydration dating of cultural artifacts. *Journal of Archaeological Science: Reports*, Vol.23, 231–242, doi: 10.1016/j.jasrep.2018.10.032.

Stevenson, C.M., Williams, C., Carpenter, E., Hunt, C.S., Novak, S.W. (2019b) Architecturally modified caves on Rapa Nui: Post-European contact ritual spaces? *Rapa Nui Journal*, Vol.32, 1–36, doi: 10.1353/rnj.2019.0005.

Stevenson, C.M., Rogers, A.K., Haverstock, G. (2023) Hydration rates for Bodie Hills obsidian regional source, based upon infrared spectroscopy and optical measurement. In: Bourdonnec, F.-X.L., Orange, M., Shackley, M.S. (Eds.), *Sourcing Obsidian: A State-of-the-Art in the Framework of Archaeological Research,* Springer Nature, Switzerland.

Stevenson, C.M., Rogers, A.K., Novak, S.W., Ambrose, W., Ladefoged, T.N. (2021) A molecular model for obsidian hydration dating. *Journal of Archaeological Science: Reports*, Vol.36, 102824, doi: 10.1016/j.jasrep.2021.102824.

Stevenson, C.M., Mazer, J.J., Scheetz, B.E. (1998) Laboratory obsidian hydration rates: theory, method, and application. In: Shackley, M.S. (Ed.), Archaeological Obsidian Studies, *Advances in Archaeological and Museum Science,* Springer US, Boston, MA, pp. 181–204, doi: 10.1007/978-1-4757-9276-8_8.

Sullivan, J.M., Twardowski, M.S., Zaneveld, J.R.V., Moore, C.M., Barnard, A.H., Donaghay, P.L., Rhoades, B. (2006) Hyperspectral temperature and salt dependencies of absorption by water and heavy water in the 400-750 nm spectral range. *Applied Optics*, Vol.45, 5294–5309, doi: 10.1364/AO.45.005294.

Zhang, X., Hu, L. (2009) Estimating scattering of pure water from density fluctuation of the refractive index. *Optics Express*, Vol.17, 1671–1678, doi: 10.1364/OE.17.001671.

Zhang, Y., Behrens, H. (2000) H2O diffusion in rhyolitic melts and glasses. *Chemical Geology,* Vol.169, 243–262, doi: 10.1016/S0009-2541(99)00231-4.

Zhang, Y., Stolper, E.M., Wasserburg, G.J. (1991) Diffusion of water in rhyolitic glasses. *Geochimica et Cosmochimica Acta*, Vol.55, 441–456, doi: 10.1016/0016-7037(91)90003-N.

Zhuravlev, L.T. (2000) The surface chemistry of amorphous silica. Zhuravlev model. *Colloids and Surfaces A: Physicochemical and Engineering Aspects,* Vol.173, 1–38, doi: 10.1016/S0927-7757(00)00556-2.